SESSION II

NOBLE GAS AND TRITIUM RETENTION

Monday, August 28, 1972
CHAIRMAN: J. A. Buckham

EXPERIMENTAL DEMONSTRATION OF THE SELECTIVE ABSORPTION PROCESS FOR KRYPTON-XENON REMOVAL
M. J. Stephenson, J. R. Merriman
D. I. Dunthorn, J. H. Pashley

MEASUREMENT OF DYNAMIC ADSORPTION COEFFICIENTS FOR NOBLE GASES ON ACTIVATED CARBON
D. P. Siegwarth, C. K. Neulander
R. T. Pao, M. T. Siegler

THE EFFECT OF HIGH PRESSURE AND LOW TEMPERATURE ON THE ADSORPTION OF XENON AND KRYPTON FROM HELIUM AND ARGON STREAMS
R. S. Ratney, D. W. Underhill

EFFECT OF RUPTURE IN A FISSION GAS HOLDUP BED
D. W. Underhill

MASS AND HEAT TRANSFER OF KRYPTON-XENON ADSORPTION ON ACTIVATED CARBON
J. L. Kovach, E. L. Etheridge

DECONTAMINATION OF HTGR REPROCESSING OFF-GASES
M. E. Whatley, R. W. Glass, P. A. Haas, A. B. Meservey, K. J. Notz

OPENING REMARKS OF SESSION CHAIRMAN:

This session is devoted to discussion of removal of xenon, krypton, and tritium from gas streams. Although to a chemist this grouping may seem a strange one, the rare gases and tritium have much in common: both are relatively abundant, long-lived (Kr-85), and of low specific biological hazard. These isotopes have become of significantly greater interest in recent years, so it is fitting that this Air Cleaning Conference begin with a discussion of rare gas and tritium removal.

EXPERIMENTAL DEMONSTRATION OF THE SELECTIVE ABSORPTION PROCESS FOR KRYPTON-XENON REMOVAL*

M. J. Stephenson, J. R. Merriman,
D. I. Dunthorn, and J. H. Pashley
Materials and Systems Development Department
Gaseous Diffusion Development Division
UNION CARBIDE CORPORATION
NUCLEAR DIVISION
Oak Ridge Gaseous Diffusion Plant
Oak Ridge, Tennessee

Abstract

Nuclear reactors and nuclear fuel reprocessing plants present different problems in terms of controlling gaseous activity discharge to the atmosphere. One gas cleaning technique potentially suitable for both cases, however, is the selective absorption process developed at the Oak Ridge Gaseous Diffusion Plant. Fundamental engineering studies, described at the 11th AEC Air Cleaning Conference, have since been followed by more specialized demonstration tests aimed at these two application areas.

I. Introduction

At the 11th AEC Air Cleaning Conference, we described some results of basic studies related to the selective absorption process for removal of krypton and xenon from nuclear process off-gas streams[3]. Those studies, aimed primarily at the feasibility and basic mass transfer aspects of the process, indicated that selective absorption has considerable potential as a gas cleaning technique and suggested guidelines for further work. During the last two years, therefore, the project has continued but with more emphasis on specific LWR system application than on fundamental characteristics of the process.

It might be recalled from the last conference that the ORGDP program was originally divided into five separate phases, viz:

PHASE I - Evaluation of absorption process performance, using refrigerant-12 as the solvent, and collection of mass transfer data.

PHASE II - Same as Phase I, except using refrigerant-11 as the process solvent.

PHASE III - Determination of the effects on the absorption process of failures in upstream air cleaning systems which result in introduction of various impurities, such as iodine, methyl iodide, and nitrous oxide, to the absorption plant.

PHASE IV - Investigation of alternative methods for permanent storage of concentrated noble gases.

*This document is based on work performed at the Oak Ridge Gaseous Diffusion Plant operated by Union Carbide Corporation, Contract W-7405-eng-26 with the United States Atomic Energy Commission.

PHASE V - Further experimental investigation of special processing situations, possibly including argon-krypton or hydrogen-krypton separations and low concentration tracer work.

The first two phases of the program were described at the previous meeting. Phase IV, dealing with handling of noble gas concentrates prepared by the absorption or some other separation process, was deleted from this project, but related work is under way at other AEC laboratories. During the past two years, then, the program has been focused on process demonstration in two areas which have been characterized recently by increasing interest: use of the absorption process to assist in treating off-gas from reactors and from fuel reprocessing plants.

Reactors and fuel reprocessing plants present very different problems, in terms of noble gas removal. On the one hand, in reactors, the noble gas activity is from both krypton and xenon, and the isotopes are present in very low molar concentrations - a few ppb to 1 or 2 ppm. On the other hand, in chemical plants, krypton-85 is the primary noble gas isotope of concern, and the krypton feed concentration is typically as high as several hundred ppm; what complicates the picture here is the potential presence in the feed of high concentrations of numerous impurities, such as oxides of nitrogen. Therefore, two separate experimental programs were conducted to demonstrate further the potential for applying the absorption technique to these two off-gas cleanup jobs. Both the reactor-oriented tests (Phase VA) and the reprocessing plant-related studies (Phase III) are described below, following a brief discussion of the process. The results of the reactor-oriented tests are presented in sections entitled *Applicability of Design Models*, *Xenon Behavior*, *Process Performance with Different Carrier Gases*, and *Miscellaneous Results*. For the fuel reprocessing plant scoping tests, sections are provided which discuss both *Calculated Impurity Behavior* and *Scoping Experiments*, including the results of laboratory experiments, pilot plant injection tests, and flow tests.

II. Process Description

A schematic flow diagram of the pilot plant is shown in figure 1. Three packed columns comprise the heart of the process. Each column is designed to exploit certain gas-liquid solubility differences that exist between the solvent and the various gas constituents that might be present. The main separation of noble gas from the bulk carrier gas is accomplished in the absorber. Here, the contaminated process gas, after being compressed and cooled, is intimately contacted with the solvent and essentially all of the krypton and xenon, along with a portion of the carrier gas, dissolves. The remaining diluent gas, depleted in contaminants, is vented from the process, while the loaded solvent is passed on to the fractionator. The purpose of the fractionator is to strip the bulk of the coabsorbed carrier gas from the loaded solvent. The fractionator is operated at a much lower pressure than the absorber, and additionally, the gas-laden liquid phase is subjected to the stripping action of counter-flowing solvent vapor. Consequently, the bulk of the less soluble carrier gases readily desorbs. The off-gas from the fractionator must ordinarily be recycled back to the absorption step, however, because it also contains a measurable amount of desorbed krypton and xenon. The enriched solvent stream produced in the fractionator subsequently passes on to the stripper. The purpose of the stripper is to produce a highly concentrated krypton-xenon gas product by driving the remaining dissolved gases from the solvent. The stripper is operated at an even lower pressure than the fractionator and with more liquid-vapor contacting to facilitate desorption of even the most soluble gases. The pure solvent leaving the stripper is pumped back to the absorber for reuse.

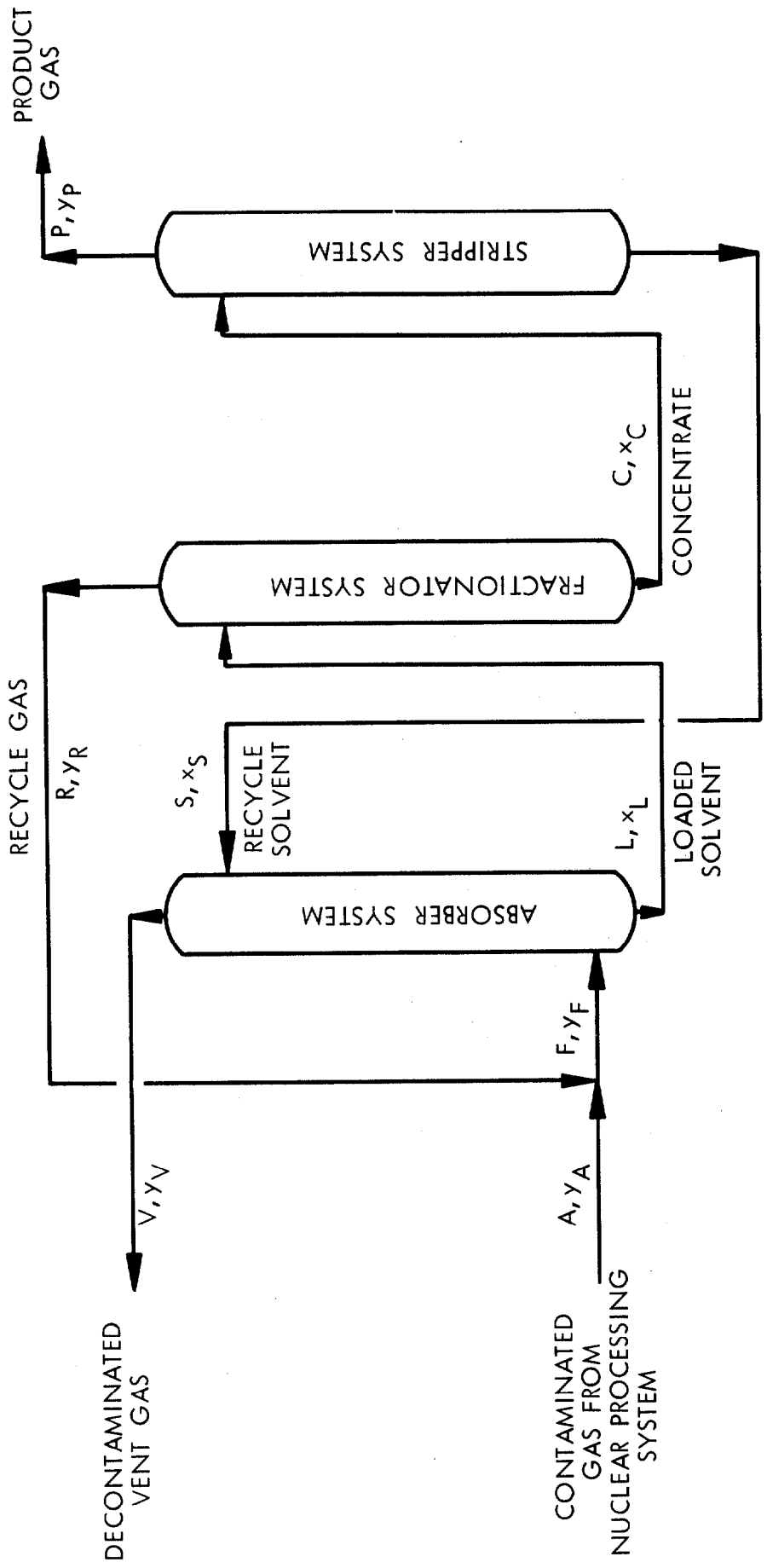

Figure 1
ABSORPTION PROCESS SCHEMATIC FLOW DIAGRAM

The development pilot plant was designed on the basis of processing a nominal 15 scfm of gas at absorber pressures as high as 600 psig and temperatures as low as minus 90°F. The pilot plant absorber and fractionator columns are 3 inches in diameter and contain 9 feet of column packing. The stripper column is 10 inches in diameter and contains 10 feet of packing.

III. Reactor-Oriented Tests

The primary purpose of reactor-related experiments was to determine how well previously developed performance correlations can be applied to situations where the concentrations of krypton and xenon in the feed gas are very low, as in reactor off-gas treatment. Other goals included experimental verification of predicted xenon behavior and testing with carrier gases other than air. Radioactive krypton and xenon isotopes were used in all tests. The results of these experiments, referred to as program Phase VA, are presented below.

Applicability of Design Models

From an engineering standpoint, particularly when fluorocarbon solvents are used, description of the mass transfer processes occurring in the absorber column is complicated by the combination of high liquid loadings, rapid mass transfer rates, multiple components being transferred, and widely varying liquid-to-gas flow ratios. In the early studies, numerous models and theories were screened, with the goal of developing an overall design package which would not only describe the data adequately but also be reasonably convenient.

Perhaps the simplest to use of the procedures investigated is the one which includes, as the stage model, a conventional film theory description. One of the design packages which we used is based on use of this model, together with an average L/V ratio, adjusted k-values, and an empirical transfer unit height correlation[3]. This system of equations, while not theoretically sophisticated in this application, is particularly convenient for repetitive calculations and, furthermore, does represent the data well enough for most design purposes. Therefore, it was decided to use this simplified design package as the basis for judging the previous correlations. The design equations from the first experimental campaign of the ORGDP program were based upon tests in which the process feeds contained relatively high levels of krypton, ranging from 40 to 8800 ppm. Although statistical analysis of the early data indicated that the transfer unit height correlations were not dependent upon feed concentrations, the low concentration tests were nevertheless performed because of substantial interest in the reactor case.

For convenience, the design procedure, which was included in our previous paper, is summarized below. Basically the model starts with the representation

$$Z = (N_{OG})(H_{OG})$$

where Z = required column height, inches;

N_{OG} = number of transfer units required to perform the stated separation; and

H_{OG} = height of the transfer unit, inches.

In the simplified case, the number of transfer units can be given by

$$N_{OG} = \frac{2.3}{1 - \frac{kG}{L}} \log\{[(y_1 - kx_2)/(y_2 - kx_2)](1 - \frac{kG}{L}) + \frac{kG}{L}\}$$

where k = effective gas-liquid equilibrium coefficient;

G/L = ratio of column average molar gas flow-to-liquid flow;

y = gas phase mole fraction of absorbing component;

x = liquid phase mole fraction of absorbing component; and

subscripts 1 and 2 refer to the gas inlet and outlet ends of the column, respectively.

The appropriate value of the effective equilibrium coefficient for the krypton and refrigerant-12 system is given by

$$k = \exp[3.8167 + 0.010197\ T]/P_{Total}$$

where T = absorption temperature, °F; and

P_{Total} = total system pressure, atmospheres.

The average L/G molar flow rate ratio for air and refrigerant-12 can be obtained from the known feed L/G molar flow rate ratio by

$$(L/G)_{avg} = 0.443\ (L/G)_{Feed}^{1.116}\ P^{0.318}$$

Finally, H_{OG} values for krypton absorption in refrigerant-12 consistent with the above can be obtained from

$$H_{OG} = \frac{1.36 \times 10^{6}\ G^{1.46}}{\alpha^{0.525}\ P^{1.74}\ L^{1.61}}$$

where H_{OG} = transfer unit height, inches;

G = column feed gas flow rate, lb/min-sq ft;

P = absorption pressure, atmospheres;

L = solvent feed flow rate, lb/min-sq ft; and

$\alpha = \exp(2.0394 - 0.008253T)$, with T in °F.

Using the run data from Phase VA krypton-air separation tests, expected krypton removals were calculated using the procedure given above and these were compared with measured values. The results are presented in table I. The measured values agree well with the calculated ones, indicating that the earlier correlations do provide a reliable framework for low concentration designs.

TABLE I

EXTENSION OF PHASE I ABSORBER CORRELATIONS
TO LOW CONCENTRATION REACTOR CASES

Run	Absorber Feed Gas*		Krypton Removal in Absorber, %	
	Flow, scfm	Krypton Content, ppb	Calculated from Correlations	Measured in Phase VA
1	5.9	150	99.8	99.89 to 99.90
2	6.1	110	99.7	99.88 to 99.89
3	5.9	130	99.7	99.88 to 99.89
4	5.9	130	99.8	99.85 to 99.86
5	5.8	130	99.8	99.91 to 99.92
6	5.9	110	99.8	99.91 to 99.92
7	6.2	70	99.8	99.86 to 99.88
8	5.9	60	99.8	99.87 to 99.89
9	4.8	50	99.8	99.92 to 99.93
10	5.0	60	99.9	99.91 to 99.93
11	5.0	50	99.8	99.90 to 99.92

* For all runs, solvent flow = 1.0 gpm, absorber pressure = 374 psia, absorber temperature = minus 25°F.

Xenon Behavior

Previous experiments involved use of krypton only, since it is the key component in absorber column design. The behavior of xenon, the key component in the stripper in many cases, had been predicted on the basis of krypton data and known solubility differences. As a part of the recent studies, however, it was decided to conduct some experiments with xenon to confirm the predicted disposition.

Eight tests were made at an absorber pressure and temperature of 374 psia and minus 25°F. Simulated process feed gas flows were between 1 and 3 scfm, and the refrigerant-12 solvent flow rate was 1.0 gpm. The carrier gas was air, which had previously been denuded of xenon. Xenon, containing xenon-133, was present in the process feed at concentrations between 3 and 15 ppb. Under these conditions, krypton removals on the order of 99.9% would be expected. Overall process xenon removal efficiencies between 99.95 and 99.99% were measured, confirming that the more soluble xenon can be absorbed at least as readily as krypton and that xenon stripping from the solvent is straightforward.

Performance with Different Carrier Gases

Since the purge or vent gases from various nuclear installations might be comprised of carriers other than air, pilot plant tests were also conducted with nitrogen, argon, helium, and hydrogen gas feeds. These tests, along with the air experiments, are summarized in table II.

It can be seen that krypton can be effectively removed from other carrier gases. As the carrier gas is changed, of course, the sharpness of the separation is affected, since the quantity of gas coabsorbed with the krypton-xenon fraction depends on the solubility of the carrier. As a consequence, changes in fractionator operation from that used in air processing are required as the carrier gas is changed. For example, more rigorous fractionation is required with argon as the carrier than with air to achieve comparable product concentrations, since argon is more soluble than air.

Miscellaneous Results

The use of radioactive isotopes in the Phase VA experiments provided an opportunity for direct measurement of krypton-xenon residence times and inventories in the process. These data are required for assessing the extent of solvent exposure to radiation. For example, the average holdup time for krypton and xenon in contact with solvent is roughly 15 minutes for processing conditions typically employed when refrigerant-12 is used as the solvent. During the Phase VA experiments, the pilot plant activity inventory ranged between 1 and 3 curies; thus the pilot plant inventory was equivalent to that of a system processing between 35,000 and 100,000 curies per year.

IV. Fuel Reprocessing Plant Scoping Tests

For fuel reprocessing plants, the behavior of feed gas impurities is of primary concern, since these not only potentially affect system operability but also determine the overall design and strategy of the krypton removal train. For this part of the program, the behavior of nitric oxide, nitrous oxide, nitrogen dioxide, carbon dioxide, methyl iodide, and iodine in a refrigerant-12 absorption system was evaluated. The evaluation included both calculations and experiments.

Calculated Impurity Behavior

Due to the lack of much definitive experimental data, the Phase III tests were preceded by calculations aimed at providing an initial indication of impurity disposition. In addition to basic physical properties, solubilities of several gaseous impurities in refrigerant-12 and other solvents were estimated using such procedures as: (a) interpolation from plots constructed using measured solubilities and Lennard-Jones constants[5], (b) a statistical thermodynamics-based estimating model[4], and (c) a molecular thermodynamics-based procedure[6].

The results of the statistical mechanics approach were found to be too sensitive to the values of the input parameters to be of consistent utility as a predictive tool, although the equation forms were used to obtain good correlations of experimental solubility data. Comparing known gas solubilities with calculated values, the other two approaches appeared to provide reasonable estimates of solubilities.

TABLE II

OVERALL PROCESS EFFICIENCIES
(Phase VA Only)

Carrier Gas	Noble Gas Contaminant	Number of Pilot Plant Tests	Process Feed*		Processing Conditions			Overall Process Efficiency, %
			Flow, scfm	Contaminant Concentration, ppb	Absorber Pressure, psia	Absorber Temperature, °F	Solvent Flow, gpm	
Air	Krypton	11	1-3	50 - 200	374	- 25	1.0	99.7 - 99.9
Air	Xenon	8	1-3	3 - 15	374	- 25	1.0	99.95 - 99.99
Nitrogen	Krypton	30	1-6	40 - 1000	314 - 422	- 35 to - 23	0.75-1.0	99.0 - 99.9
Argon	Krypton	6	1-4	10 - 1400	374	- 25	1.0	99.0 - 99.7
Helium	Krypton	9	2-7	100 - 4300	254 - 374	- 40 to - 25	0.75-1.0	99.4 - 99.9
Hydrogen	Krypton	3	1-2	300 - 600	194	- 25	0.75	99.0 - 99.9

* The process feed plus the fractionator recycle make up the absorber feed.

The calculations indicated that the gaseous impurities can generally be grouped into three categories:

1. Very soluble components, such as carbon dioxide and nitrous oxide, that follow krypton and xenon through the process and ultimately concentrate in the stripper off-gas or product stream;

2. Slightly soluble components, such as methane and nitric oxide, that follow nitrogen and oxygen through the process and similarly distribute between the absorber vent and product*; and

3. Relatively insoluble components, such as hydrogen and helium, that pass through the absorber and are subsequently vented.

For the condensed liquids and desublimed solids, i.e., methyl iodide, nitrogen dioxide, and iodine, estimates of behavior were made considering solubilities in similar systems. For example, iodine is known to form solutions with several fluorocarbons[1].

On balance, then, the calculations and available data indicated that the impurities could probably be handled in the absorption process.

Scoping Experiments

Using the above estimates as guides, the scoping tests were next conducted. These tests included a few laboratory screening experiments, pilot plant tests in which various gases were sequentially injected, and runs in which mixtures of impurities were continuously introduced into the system. In several tests, krypton-85 was included so that the process separation performance could be monitored in the presence of impurities.

Laboratory screening tests were conducted with nitric oxide, methyl iodide, and iodine. For nitric oxide, an infrared cell experiment showed that the rate of reaction with oxygen is large enough for nitric oxide to essentially disappear during processing in the absorption system, as expected. For methyl iodide, tests conducted at minus 20°F indicated that the compound is miscible with refrigerant-12. And, in the case of iodine, experiments at minus 20°F showed that iodine forms a violet solution with refrigerant-12, with a solubility on the order of 0.1 mole percent.

For the injection experiments, the pilot plant was operated in a total recycle mode, with the absorber column at 374 psia and minus 25°F. Krypton and xenon were present at concentrations near 20 and 100 ppm, respectively, in the simulated process feed gas. Carbon dioxide, nitrous oxide, nitric oxide, and nitrogen dioxide were sequentially injected into the pilot plant, and the concentrations were gradually built up by repeated additions. The target concentrations were in the high ppm to low percent range in the feed gas. No operational problems were encountered and the overall krypton removal efficiency remained at the initial high level (greater than 99%). Analyses of the gas streams showed that nitrous oxide and carbon dioxide had followed krypton and xenon and that nitric oxide had disappeared to below the limit of detection. Nitrogen dioxide was not found in analyses of the gas streams, indicating that it had remained in the liquid.

* However, based on consideration of kinetic data and the temperatures and pressures prevailing in the absorption system, it was estimated that most nitric oxide in the system would be rapidly converted to nitrogen dioxide in the presence of air.

For the flow tests, the pilot plant was operated, as shown in figure 2, with a continuous air feed, and with the columns vented. In the first run, carbon dioxide, nitrous oxide, nitric oxide, and nitrogen dioxide were metered to the process in amounts giving impurity feed concentrations of several hundred ppm to nearly 1%. This particular mode of plant operation was maintained for two weeks. Carbon dioxide and nitrous oxide, as observed before, absorbed readily in the refrigerant-12 solvent, followed krypton and xenon, and were concentrated in the stripper off-gas. Again, nitric oxide was not detected in either the process off-gas or solvent, indicating essentially complete conversion to nitrogen dioxide. Based on both gas and liquid sample results, nitrogen dioxide, on the other hand, dissolved in the solvent and began accumulating there from the onset of the run. Eventually, corresponding to the buildup in the liquid, small quantities of nitrogen dioxide began appearing in the process off-gas. With 1 to 2 mole percent nitrogen dioxide in the solvent, less than 5 ppm was detected in the absorber off-gas. Later, with 5 to 10 mole percent in the solvent, approximately 200 ppm was detected in the absorber off-gas, and additionally, about 20 ppm was found in the stripper off-gas. As before, no operational difficulties occurred.

A similar pilot plant test was conducted with iodine and methyl iodide. Each material was fed to the plant over a 2-day period. The test data showed that these compounds tend to remain in the solvent and that iodine inadvertently released to the krypton removal system should be contained there and not be further released to the atmosphere.

A summary of the impurity scoping tests is given in table III. Based on these tests, it definitely appears that the krypton absorption process is capable of efficient operation with contaminated feeds of the type likely to be encountered in fuel reprocessing plants in the case of failures of upstream air cleaning devices. Furthermore, it is apparent that, with the proper specification of the process auxiliaries, the absorption system could be designed for sustained operation with a continuous feed containing the above impurities.

V. Plans for Future Work

The ORGDP noble gas absorption program, since its inception in FY 1967, has been oriented mainly toward LWR-related applications - either reactors or chemical plants. With the completion of the work outlined in this paper, we believe it is appropriate to bring the LWR-related portion of our development program to a close. In the framework of what a development program is able to accomplish, many of the basic process questions have been answered, and the technical potential for process application, at least, has been demonstrated. Consequently, no more development work specifically for LWR systems is planned. This decision is supported by the fact that there is now beginning to be some commercial interest in the process[2].

A new program involving the selective absorption process, beginning in FY 1973, is being initiated. This new program, which is being conducted jointly with ORNL, has the objective of defining and demonstrating a total krypton removal package for an LMFBR fuel reprocessing plant off-gas treatment system.

A schematic flow diagram is given in figure 3 for a complete krypton absorption plant, reflecting how the process might be applied in this case. The plant includes not only the main columns but also certain auxiliaries. The feed preparation system includes equipment required for drying, filtering, and otherwise conditioning the feed gas. The solvent recovery system removes solvent vapors from the absorber column off-gas stream (process vent). Alternatives being considered here for refrigerant-12 service include cooling-condensing, either directly or using an

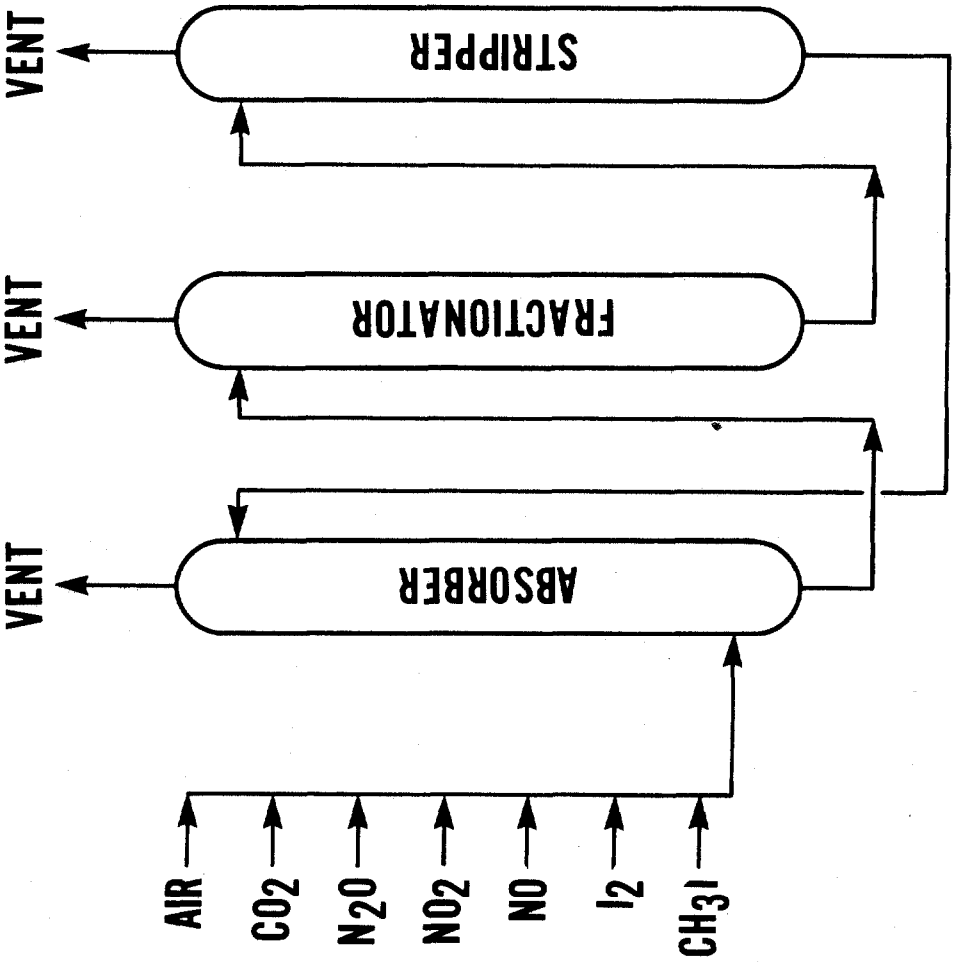

Figure 2
FLOW SCHEMATIC FOR IMPURITIES SCOPING TESTS

TABLE III

SUMMARY OF IMPURITY SCOPING TESTS

Impurity	Concentration In Process Feed, ppm	Disposition in Process	Effect on Plant Operability	Effect on Krypton Removal Efficiency	Influence on Plant Design
Carbon Dioxide	1,000 - 3,500	Follows krypton-xenon	None	None	Carbon dioxide trap in krypton product line
Nitrous Oxide	1,000 - 6,700	Follows krypton-xenon	None	None	Nitrous oxide trap in krypton product line
Nitrogen Dioxide	100 - 600	Accumulates in solvent	None, unless solubility limits are exceeded	None	Solvent purification system
Nitric Oxide	1,000 - 2,000	Converts rapidly to nitrogen dioxide	Same as nitrogen dioxide	Same as nitrogen dioxide	Same as nitrogen dioxide
Iodine	50 - 100	Plates out on surfaces and accumulates in solvent	None, unless solubility limits are exceeded	Not determined	Specially designed gas heat exchanger and solvent purification system
Methyl Iodide	100 - 200	Accumulates in solvent	None	Not determined	Solvent purification system

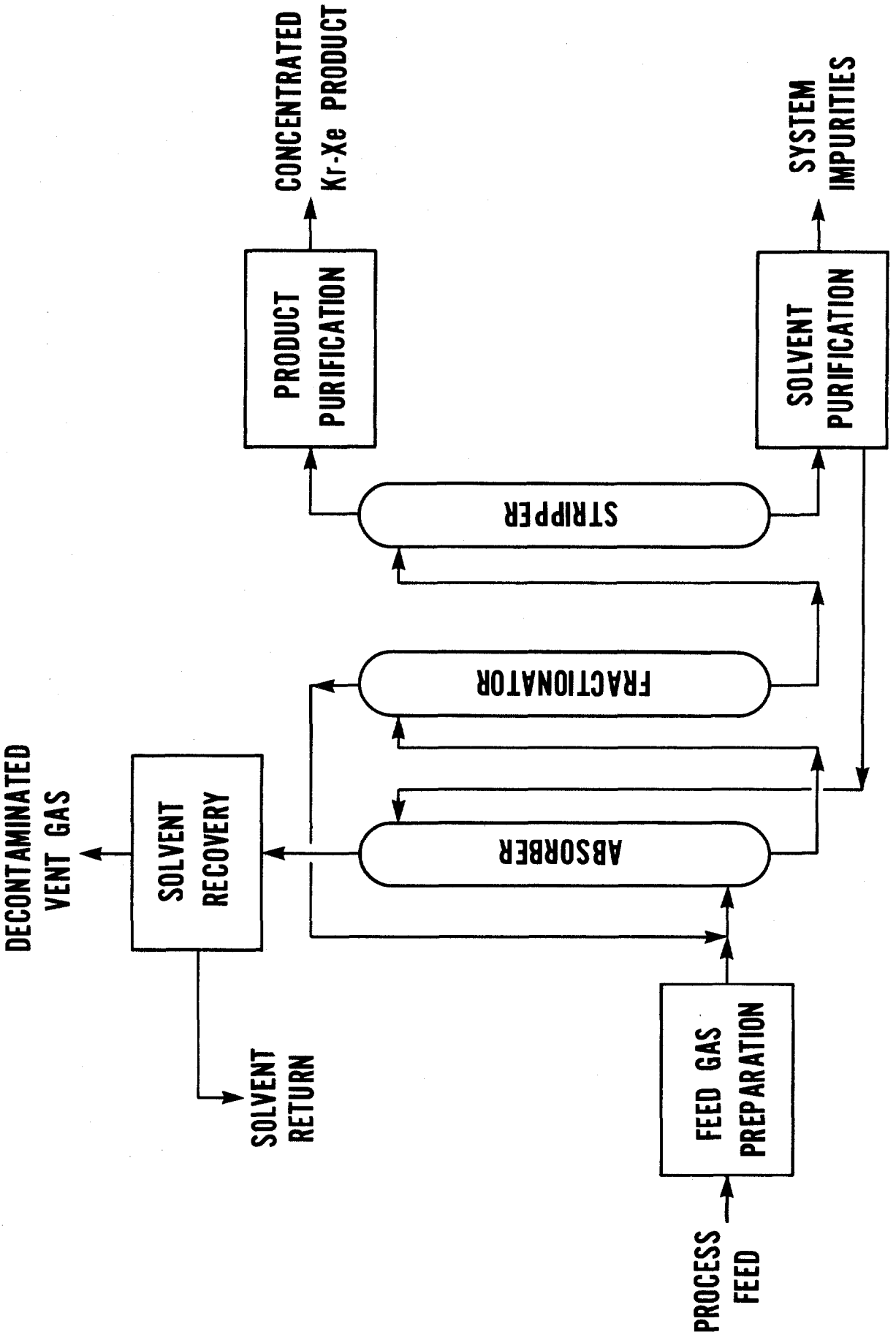

Figure 3
SCHEMATIC FLOW DIAGRAM OF A COMPLETE ABSORPTION PROCESS

isentropic expansion, adsorption, using 5A molecular sieves, and a combination of these two operations. The solvent purification system is designed to control the accumulation of impurities which remain in the liquid phase. These include iodine, methyl iodide, nitrogen dioxide, heavy hydrocarbons, and the high boiling refrigerant-12 degradation products, refrigerant-114 and refrigerant-113. Finally, the purpose of the product purification system is to scavenge nitrogen, oxygen, nitrous oxide, refrigerant-12, and carbon dioxide from the already low flow rate stripper off-gas, resulting in an essentially pure, highly concentrated noble gas product stream.

During the next two years, these auxiliary systems will be designed, built, and added to the ORGDP pilot plant. The total package will then be operated for extended periods of time. The primary purpose of the work will be to establish the long-term operability and performance of a complete system when processing a feed containing typical LMFBR fuel reprocessing plant concentrations of numerous impurities, such as carbon dioxide, nitrogen oxides, light organics, heavy organics, iodine forms, ozone, particulates, etc. Also, impurity concentration limits above which the process malfunctions will be defined. Based on the scoping tests described today, we are optimistic about the chances of success of the new program.

VI. Conclusion

During the past two years, many of the specific questions raised concerning application of the selective absorption process to reactors and fuel reprocessing plants have been successfully answered, thereby supplementing earlier work which was of a more general nature. For example, the recent data show that the process can be operated efficiently at low concentrations of krypton, as well as at high levels; can remove xenon at least as effectively as krypton; and can separate the noble gases from carrier gases other than air. Also, the process continues to separate krypton efficiently when the feed becomes contaminated with nitrogen oxides and carbon dioxide and, in fact, has a high tolerance for these impurities. Furthermore, it appears that any iodine and methyl iodide passing into the system collect in the solvent and could be removed from the liquid stream, if desired, by treatment of the recycle solvent.

When these development program results are considered along with the earlier results of the program, then the application of the process to a variety of gas cleaning jobs continues to seem very promising.

References

(1) Hildebrand, J. H., and Scott, R. L., *Regular Solutions*, Prentice-Hall, Inc., New Jersey (1962).

(2) Hogg, R. M., "New Radwaste Retention System", *Nuclear Engineering International*, *17*:189, 89-99 (1972).

(3) Merriman, J. R., et al., *Removal of Radioactive Krypton and Xenon from Contaminated Off-Gas Streams*, Union Carbide Corporation, Nuclear Division, Oak Ridge Gaseous Diffusion Plant, August 1970 (K-L-6257).

(4) O'Connell, J. P., and Prausnitz, J. M., "Applications of Statistical Mechanics", *Ind. Eng. Chem.*, *60*:1 (January 1968).

(5) Prausnitz, J. M., *Molecular Thermodynamics of Fluid-Phase Equilibria*, Prentice-Hall, Inc., New Jersey (1969).

(6) Yen, Lewis Chinsun and McKetta, J. J., Jr., "A Thermodynamic Correlation of Nonpolar Gas Solubilities in Polar, Nonassociated Liquids", *A.I.Ch.E. Journal*, *8*:4 (September 1962).

DISCUSSION

KOVACH: Have you operated the system in a once-through mode, or was it a recycled mode operation?

STEPHENSON: For which application? The impurities work, or the reactor-operated studies?

KOVACH: The reactor-operated studies.

STEPHENSON: We've operated in both modes; once-through and recycle.

KOVACH: The other two questions I have are: Have you tried it with krypton and xenon simultaneously? Have you tried to evaluate with radioactive iodine or methyliodide the possibility of an isotope exchange between Freon and ^{131}I?

STEPHENSON: We do not have the capability of analyzing multi-isotope mixtures because our analytical equipment cannot handle the two components. We can only look at one isotope at a time. We have done air separation studies in which we have used normal krypton and normal xenon. There appeared to be no interference between the two gases.

As regards radioactive iodine and methyliodide, we have not looked at that as yet, although I do not expect an exchange of an iodine molecule for chlorine or fluorine because the carbon to fluorine and carbon to chlorine bonds are much stronger than you would expect for carbon to iodine. You would not expect a cleavage of that bond in preference for a carbon-iodine.

KOVACH: In methyliodide removal work, when evaluating various impregnants on activated carbon, it was found that methyliodide exchanges with bromine and chlorine, and to some extent with fluorine also.

STEPHENSON: Bromine I might expect, but I don't believe that we would expect exchange with chlorine and fluorine.

KOVACH: It was to a smaller degree, but there was some exchange.

STEPHENSON: Well, you might get it to a small degree, but I wouldn't expect anything significant, since those bonds are very strong.

BURCHSTED: Do you know the effect of high radiation level on the solvent, or on the interaction of impurities, or on the trapping efficiency of the process at, say, 10^8 rad?

STEPHENSON: Looking first at the effect of high radiation levels, one advantage of our system is that the holdup is very small, i.e., the amount of noble gas in the system is small. So, you would never expect an accumulation of enough radiation in the system to result in the exposure that you were talking about.

BURCHSTED: Wouldn't there be high radiation levels in the feed gas itself?

STEPHENSON: Yes, but there's only about a 15-minute residence time from the point where the feed enters the process to where it's collected in the product. Consequently, the actual inventory of radioactive material in contact with the solvent is small.

MEASUREMENT OF DYNAMIC ADSORPTION COEFFICIENTS FOR NOBLE GASES ON ACTIVATED CARBON

D. P. Siegwarth, C. K. Neulander, R. T. Pao, and M. Siegler
Nuclear Energy Division
General Electric Company
San Jose, California

Abstract

Experimental techniques and analytical procedures were developed to measure the noble gas dynamic adsorption coefficients on activated carbon with a continuous inlet noble gas flow rather than the normal radioactive tracer pulse injection method. Nonradioactive krypton or xenon was blended with dry air to a concentration of 1 to 10 ppm by volume and continuously fed to the inlet of the test adsorber. The adsorber effluent was divided to permit sample storage as well as real-time analyses. The experimental work was performed with 1-1/4- or 2-in. diameter adsorber columns 2 to 8 ft long.

To measure a few parts per million of krypton or xenon in air, special analytical techniques were developed to pre-concentrate the samples. The breakthrough curves were established by quantitatively measuring the adsorbate concentration in the carbon adsorber effluent with an ultrasonic detector gas chromatograph. The dynamic adsorption coefficients (k_d) were calculated from:

$$k_d = F\, t_m / M$$

where k_d = dynamic adsorption coefficient [cc(20°C, 1 atm ≡ STP)/gm] ; F = gas flow rate [cc(STP)/min] ; t_m = adsorbate mean residence time (min); M = mass of dry carbon (gm).

The experimentally determined dynamic adsorption coefficients were in close agreement with those previously reported in the literature for other carbons. The equilibrium stage theoretical model adequately described the measured breakthrough curves.

I. Introduction

Removal of noncondensable gases from the turbine condensers in thermal generating plants is generally accomplished with steam jet air ejectors (SJAE). In nuclear generating plants, the radioactive noble gases Kr and Xe are a potential source of radioactivity in the plant gaseous effluents. Unless properly treated, the noble gases could become a major source of off-site radiation. Since most Kr and Xe radioactive isotopes have relatively short half-lives, systems which delay the noble gases can be used effectively to reduce the total activity by radioactive decay.

The SJAE effluent (offgas) from a boiling water reactor is composed primarily of hydrogen and oxygen from the radiolysis of reactor water and air from condenser in-leakage, but also contains trace amounts of radioactive noble gases. General Electric is offering recombiner – activated carbon systems designed to delay the noble gases and also is developing methods for the removal and storage of these gases. Measurements of the noble gas concentrations in the recombined offgas (normally 0.5 to 1.5 ppm by volume) and evaluation of different noble gas delay or removal systems required the development of new analytical and experimental methods. These methods and their application to the evaluation of activated carbon as an adsorbent for Kr and Xe are discussed.

II. Theory

The dynamic adsorption process is one in which a gaseous species in a flowing carrier gas stream is physically adsorbed onto the surface of a solid adsorbent. Although the adsorbate is not bound permanently to the adsorbent, its exit from the adsorption bed is delayed with respect to the carrier gas. Several theoretical treatments have been used to characterize the dynamic adsorption process, and the one developed at the Oak Ridge National Laboratory (ORNL) has been adopted for this paper.[1] In this approach, the packed adsorber column is assumed to be divided into a number of theoretical chambers in series. The gas flow into each chamber is instantly distributed and brought to adsorption equilibrium.

A mass balance for the adsorbate across each of the N stages is

$$\frac{dy_i}{dt} = -\frac{FN}{k_d M}(y_i - y_{i-1}) \tag{1}$$

where

y_i = Volume fraction of adsorbate in gas phase leaving the i^{th} stage at time t;
F = Total gas flow rate [cc(20°C, 1 atm ≡ STP)/gm]
M = Total charcoal mass on dry basis (gm);
N = Number of theoretical equilibrium stages;
t = Time (min).
k_d = Dynamic adsorption coefficient [cc(STP)/gm]

Solution of the series of N differential equations with the appropriate adsorbate initial boundary conditions yields the effluent concentration profile from the N^{th} stage. For a unit input pulse at t = 0, this solution is

$$y_N = \frac{N^N F^{N-1} t^{N-1}}{(N-1)!\,(k_d M)^N} \exp\left(\frac{-NFt}{k_d M}\right). \tag{2}$$

By differentiating Equation (2) with respect to time and setting the result equal to zero ($y'_N = 0$) the time, t_{max}, required for the concentration to reach a maximum, y_{max}, is

$$t_{max} = \frac{(N-1)\,k_d M}{NF}. \tag{3}$$

It has been shown that for a linear adsorption isotherm, which should apply at low adsorbate concentrations, the mathematical solution to a step change (constant input) initial boundary condition is equivalent to the integral of the solution for a square wave (pulse) boundary condition;[2] i.e.,

$$z_N = \int_0^t y_N\, dt \tag{4}$$

where z_N provides the effluent concentration profile for a step constant input.

Thus, the time required to reach the peak maximum for the pulse case, t_{max}, (obtained from $y'_N = 0$) can be equated to the time to the inflection point in concentration for constant input (since $z''_N = y'_N$). For the near-symmetrical effluent distribution function described by Equation (2), this time can be denoted by t_m, the mean residence time of the adsorbed species in the column, without serious error.

For long, well-packed beds, N will be a large number, so that (N-1)/N will be approximately unity. The assumption of large N and substitution of t_m for t_{max} in Equation (3) yields

$$t_m = k_d M/F. \tag{5}$$

This result shows that a characteristic residence time of an adsorbed species in a dynamic adsorption column of mass M and at carrier-gas flow rate F is defined by the proportionality constant, k_d. Once the effect of those system parameters which affect k_d are known, the mean delay time for any given total flow (F) and adsorber size (M) can be calculated by using Equation (5).

A computer program was written to integrate Equation (2) numerically. The number of equilibrium stages (N) was calculated by using the revised correlation proposed by Vermeulen, as described by Robell and Merrill.[2] Effluent profiles were calculated by integrating Equation (2) after substituting the experimental conditions and the value of N found above. The profiles agreed well with the experimentally measured curves over a wide range of conditions (Section V), which lends credence to the application of the equilibrium stage theory to dynamic noble gas adsorption on carbon.

III. Analytical Technique

Analytical Equipment

An analytical instrument capable of detecting the noble gases in air at the parts per million level and below was needed for analyzing actual and simulated reactor offgas. Since the instrument would be used both in the laboratory and in the field, it also had to be somewhat portable. A survey of available analytical techniques indicated that a gas chromatograph (GC) with a helium ionization detector (HID) or an ultrasonic detector (UD) could probably meet these requirements.

The HID is at least an order of magnitude more sensitive than the UD. However, the high sensitivity of the HID requires the chromatographic system be extremely clean and free from leaks, i.e., water vapor or air can swamp the detector. In fact, the sensitivity of the HID to leaks precludes the use of any valving between the sample inlet and HID. Previous experience with an HID GC showed the detector was easily poisoned and required hours of bake-out time after minor maintenance or instrument modifications (e.g., column changes). In addition, the instrument was quite delicate and subject to shipping damage. The UD has the advantages of a wide dynamic range (10^6); freedom from single carrier gas requirement, i.e., the HID requires ultra-pure helium carrier; flexibility, since column switching valves can be used; and predictable calibration. Based on these comparisons, it was decided to purchase a GC with the more rugged and flexible UD.

The UD system measures the changes in the speed of sound in gas mixtures by comparing the phase shift of a signal traversing the mixture to a reference signal. The characteristics of the UD have been discussed by Noble, et al.,[3] Todd and DeBord,[4] and Grice and David.[5] As shown by Grice and David,[5] the peak area for a particular sample component in degree-seconds (A) for a given detector can be approximated by

$$A = Kn(M - M_c)/PF_c \qquad (6)$$

where

- K = Detector constant;
- n = Moles of component in sample;
- M = Molecular weight of component;
- M_c = Molecular weight of carrier;
- P = Pressure of gas in detector cell; and
- F_c = Carrier flow rate.

For a given set of chromatographic conditions, the pressure and flow rate are constant. Thus, the response per mole is a function of the molecular weight difference, $M - M_c$. Equation (6) indicates that when using hydrogen or helium as a carrier gas, a single calibration curve can be used without appreciable error for all samples except those of very low molecular weight. The data reported by Grice and David[5] illustrate these predictions are valid.

Column Development

As shown in Figure 1, it is not difficult to separate Kr from air with a 5A molecular sieve (MS) column when the relative concentrations of O_2, N_2, and Kr are within a few orders of magnitude of each other. However, the quantitative determination of 1 ppm Kr in air (Figure 2) presents a more difficult problem. The Kr peak appears on the tail of the O_2 peak and is too small for accurate quantitative measurements. An experimental investigation of several GC column packing materials and operating conditions was conducted to optimize the separation of trace quantities of Kr and Xe from air. The results of this program (Table 1) indicated that Carbosieve-B provided good separation between air, Kr, and Xe, but suffered from interference of CH_4 and CO_2. Porapak-T appeared capable of separating Xe from CO_2, CH_4, and air. Type 5A-MS at subambient temperature (-10 to 10°C) was the best for the Kr analysis. In the final analytical scheme, a Carbosieve-B column was incorporated to eliminate most of the N_2 and O_2 from the sample, followed by a 5A-MS column for Kr analysis or a Porapak-T column for Xe analysis.

Analytical Procedure

A Tracor Model MT-150 GC equipped with a dual UD (Figure 3) is used to detect the sample components, and the corresponding peak areas are measured with an Autolab System IV computing integrator. The required sensitivity is obtained by using 20 cc air samples. Most of the air is separated from the sample in a cutting column; the final separation is effected in

one of two analytical columns (Figure 4). Helium carrier gas (99.995% purity) is first passed through a 1/4-in. diameter by 10-ft long activated carbon column maintained at liquid nitrogen temperature to remove any remaining contaminants. Valve V1 is used to select a sample either from a 20 cc sample loop or from the sample storage system described in Section IV. The sample is injected into a Carbosieve-B cutting column. The Kr and Xe are preferentially retained on the Carbosieve-B, and the bulk of the air is vented through valve V3 and needle Valve N3. After venting the air, valve V3 is used to direct the flow through valve V2 to the 5A-MS column and Detector-A for the Kr analysis, and to the Porapak-T column and Detector-B for the Xe analysis.

The pressures and flows throughout the system are balanced to minimize flow disturbances caused by the valve switching operations during the analysis. The GC operating conditions are shown in Table 2. The normal analysis time is 18 to 20 minutes. As shown in Figure 5, good separation is achieved between the Kr and N_2 peaks. Figure 6 shows that a reasonably sharp Xe peak is also obtained.

TABLE 1. Gas Chromatograph Column Development
(Carrier Gas – Helium)

Packing Material	Carrier Flow [cc(STP)/min]	Column Temperature (°C)	Column Length (ft)	Comments
Activated Carbon	80	27 to 80	2	CH_4 in air interferes with Kr peak.
Carbosieve-B	35 to 60	30	4	CH_4 interferes with Kr, and CO_2 interferes with Xe.
5-A Molecular Sieve	30	−15 to 95	8 to 12	At −10 to 10°C, can be used for Kr. Interference from H_2O and CO_2 for Xe.
Porapak-Q	25 to 70	−40 to 27	8 to 12	Insufficient separation between air and Kr. Water and CO_2 interfere with Xe.
Porapak-T	40 to 70	27 to 120	12	Insufficient separation between air and Kr. Good for separating Xe from air, CO_2 and CH_4.

TABLE 2. Gas Chromatograph Operating Conditions

	Krypton	Xenon
Carrier Flow, cc(STP)/min.	60	60
Detector		
Pressure, psig	30	30
Temperature, °C	120	120
Cutting Column		
Length, inches	9	9
Inside Diameter, inches	0.17	0.17
Packing	Carbosieve-B	Carbosieve-B
Mesh Size	140/200	140/200
Analytical Columns		
Length, ft	8	12
Inside Diameter, inches	0.10	0.10
Packing	5A-MS	Porapak-T
Mesh Size	60/80	50/80
Temperature, °C	−10 to +10	0 to 30

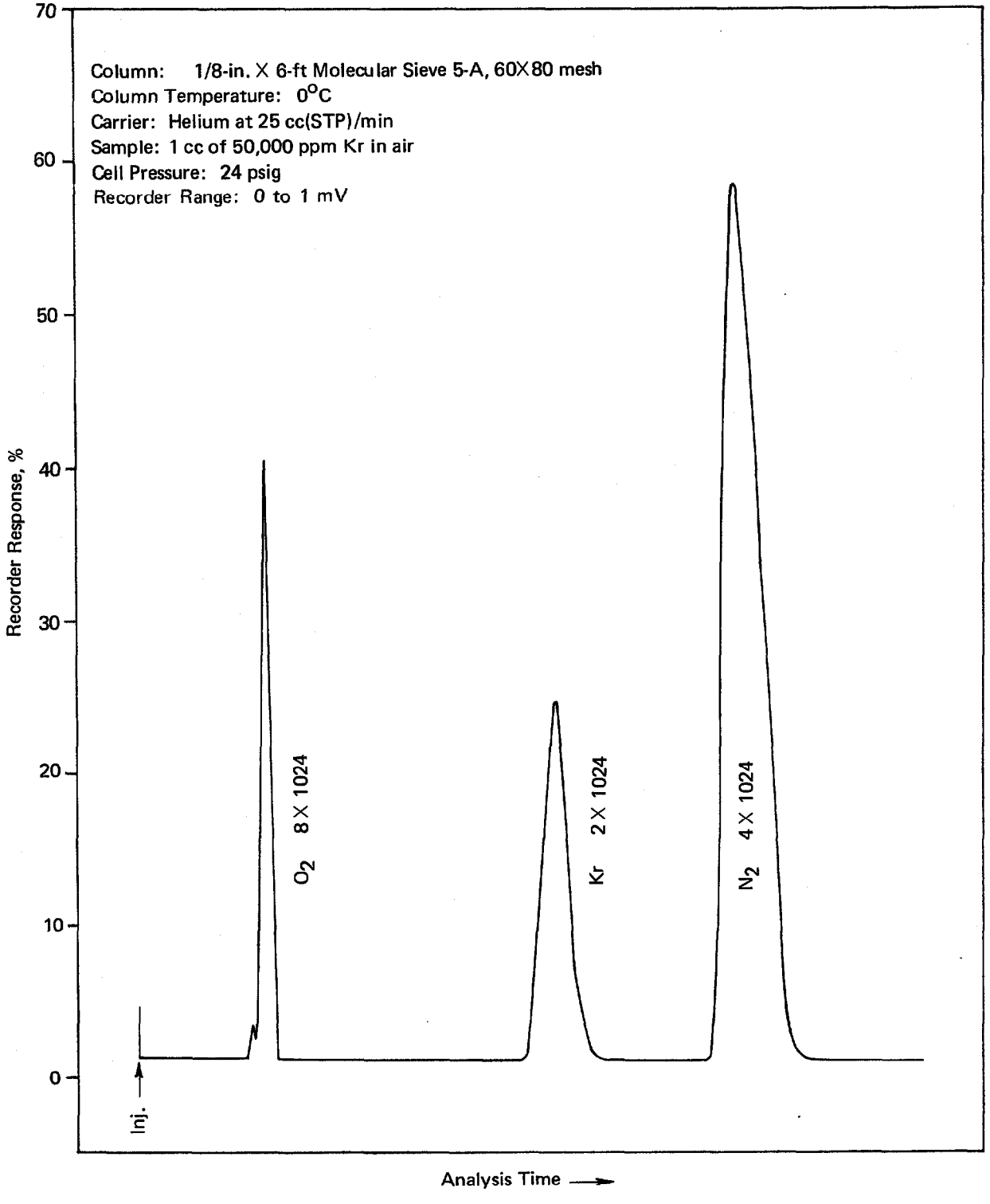

FIGURE 1. SEPARATION OF OXYGEN, KRYPTON, AND NITROGEN

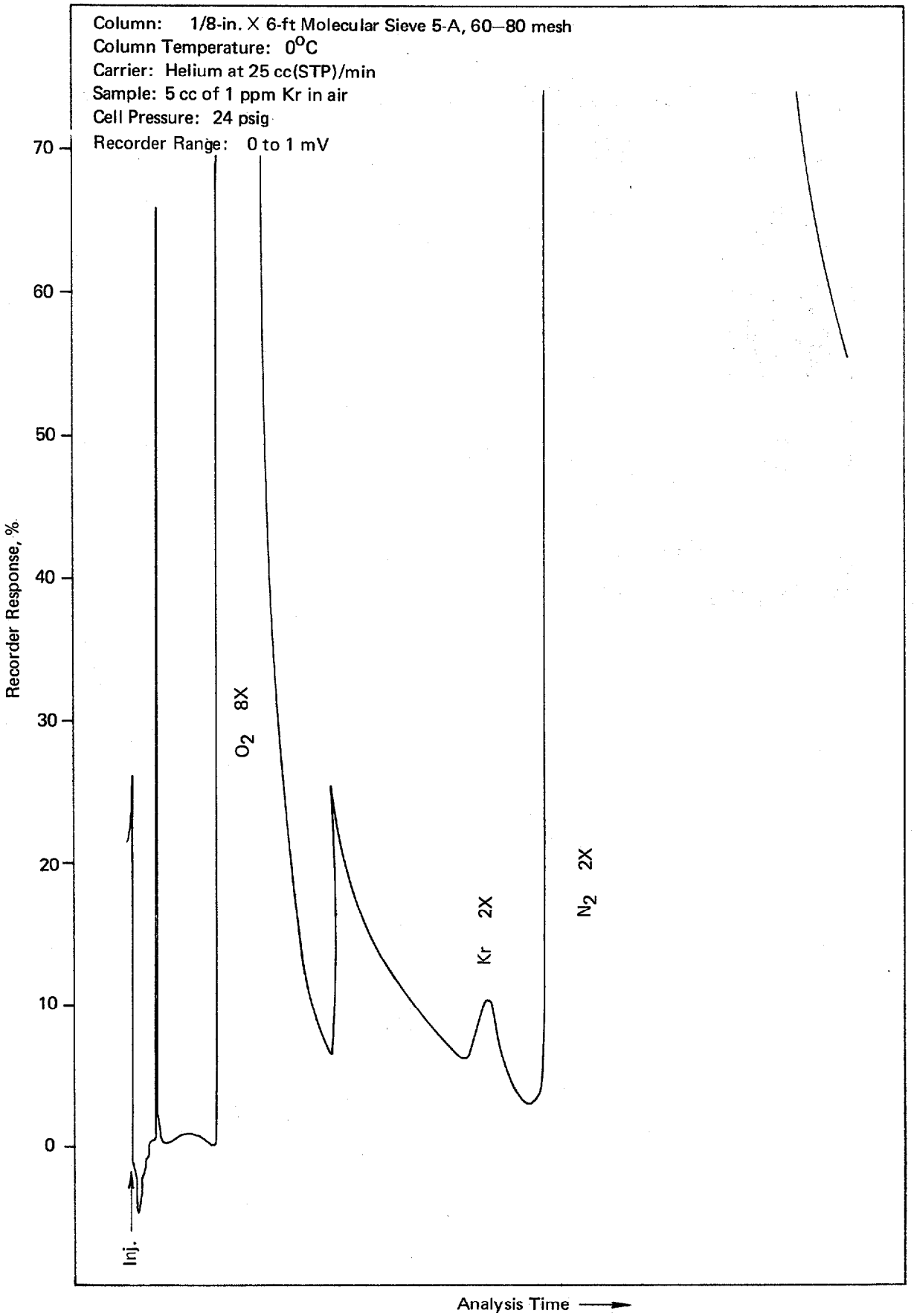

FIGURE 2. DETERMINATION OF 1 ppm KRYPTON IN AIR

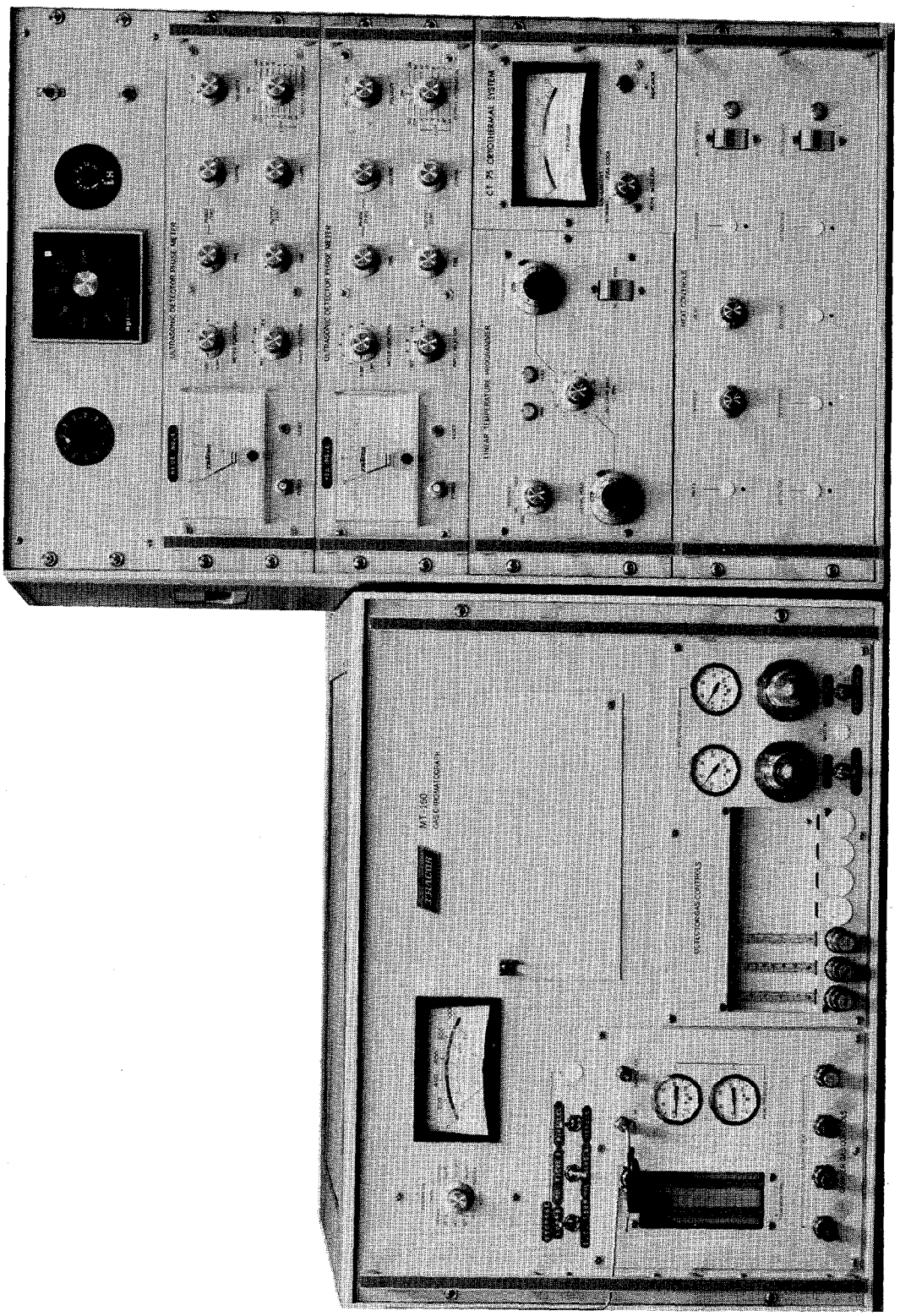

FIGURE 3. TRACOR MT-150 GAS CHROMATOGRAPH

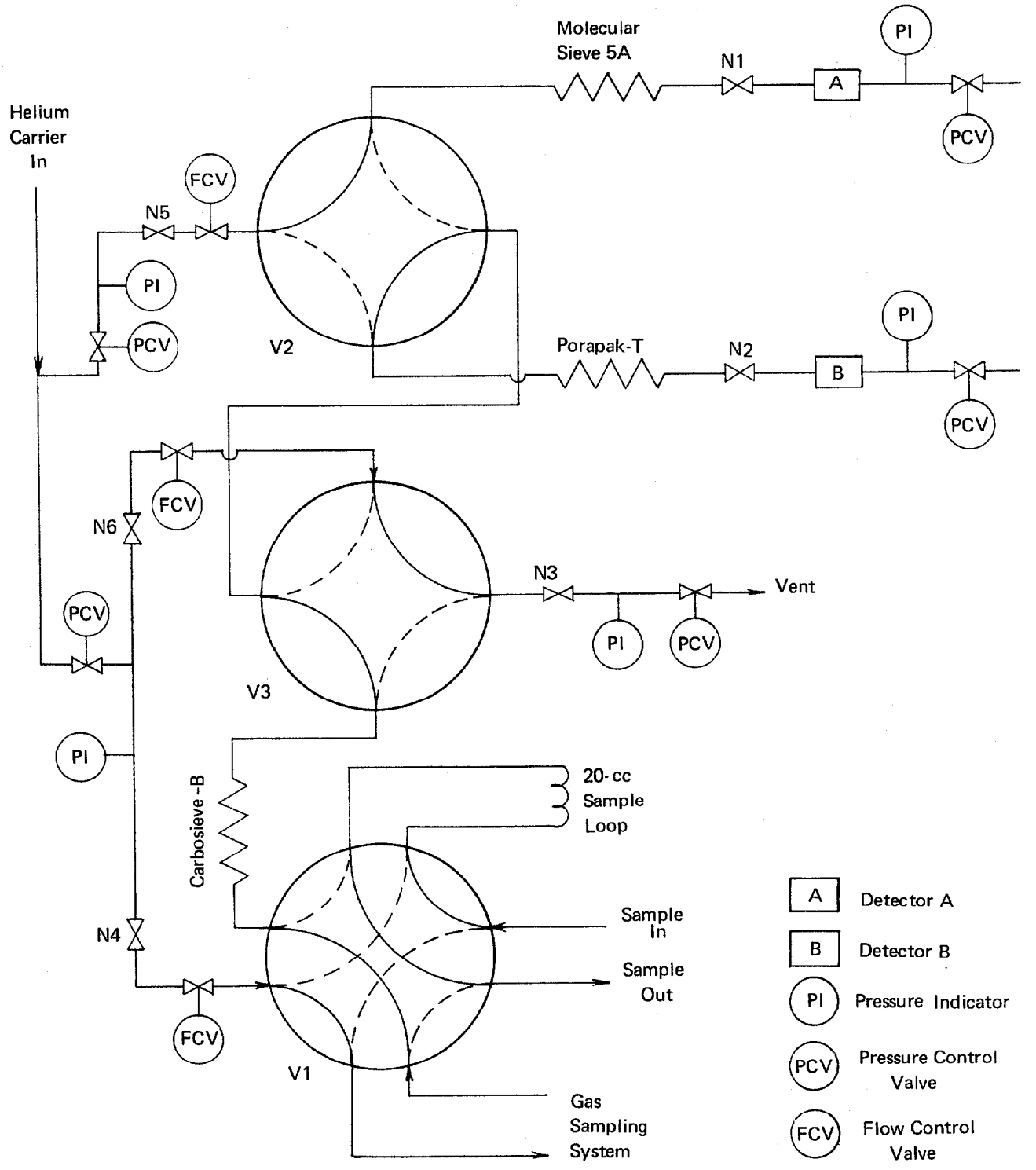

FIGURE 4. GAS CHROMATOGRAPH FLOW DIAGRAM

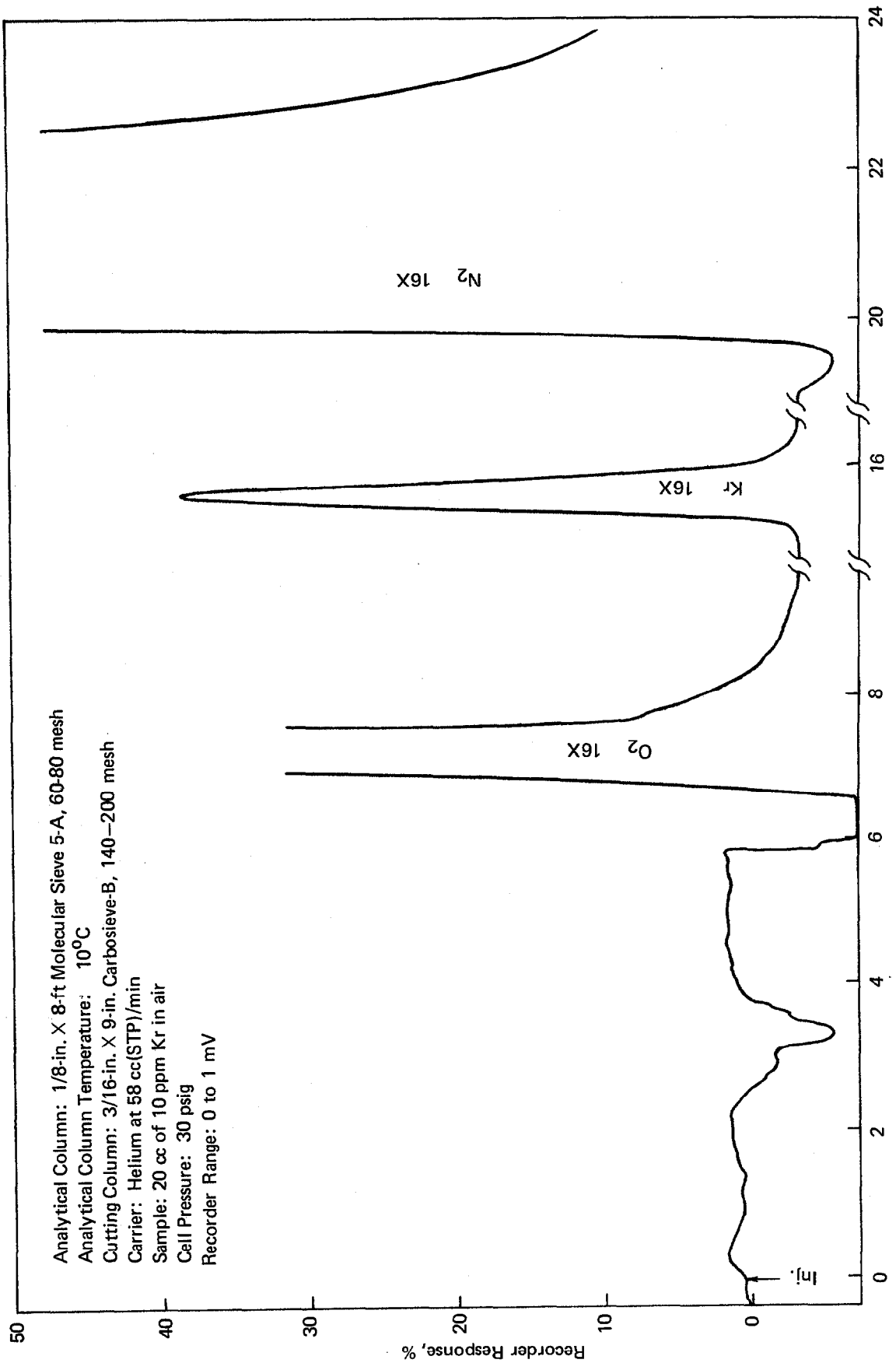

FIGURE 5. TYPICAL KRYPTON ANALYSIS

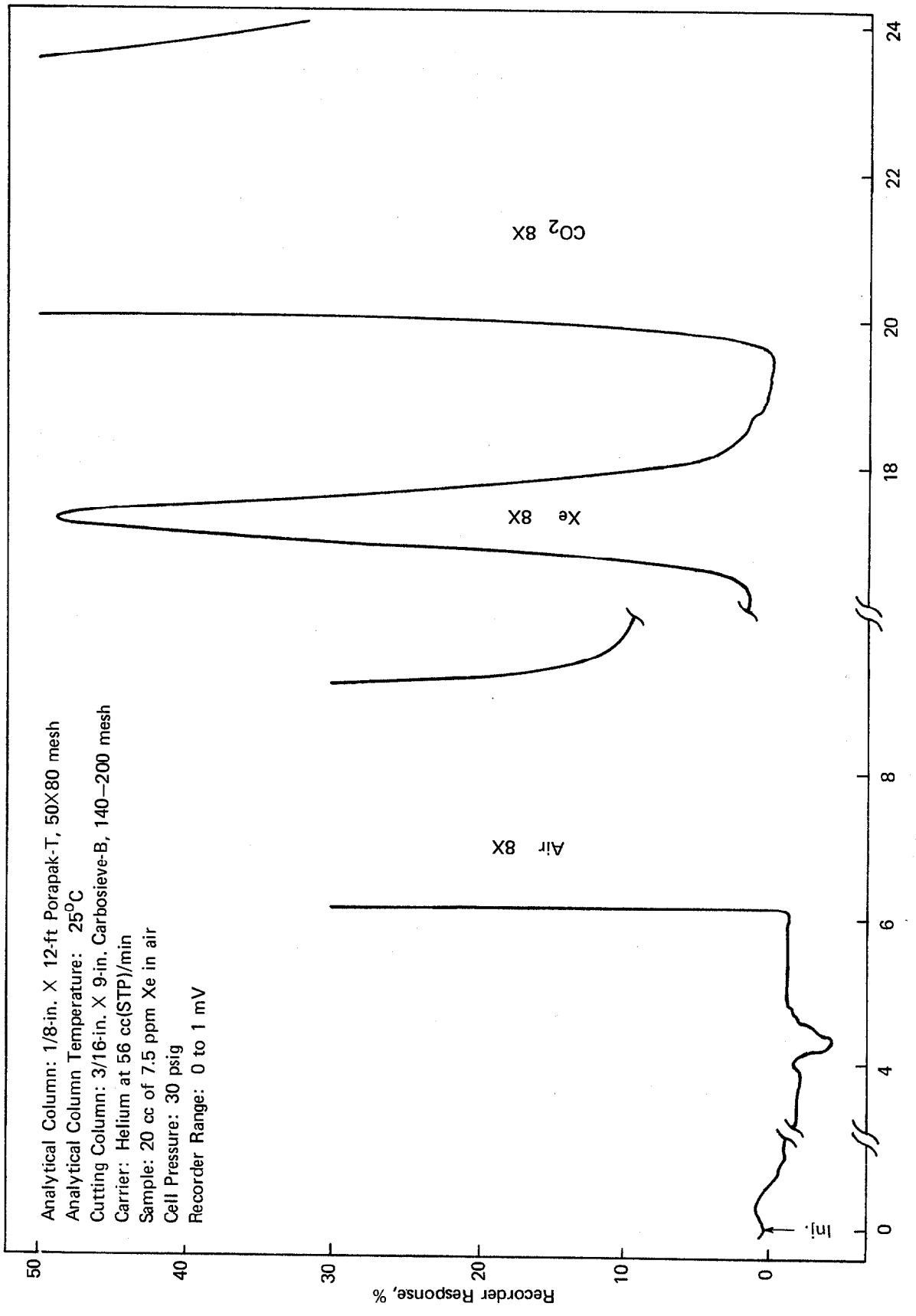

FIGURE 6. TYPICAL XENON ANALYSIS

IV. Experimental Apparatus

Flow System

The dynamic adsorption experiments have been performed with the equipment shown schematically in Figure 7. Compressed or cylinder air is dried to an inlet dewpoint of -70°C (< 3.5 ppm moisture) with Type 3A-MS (to prevent holdup of CO_2) and is cleaned of trace hydrocarbons with an activated carbon filter before being blended with a prepared run mix containing 100 to 500 ppm of Kr or Xe in zero-grade air (< 2 ppm hydrocarbon content). The two gas flows are individually metered through critical flow orifices to give noble gas concentrations of 1 to 10 ppm at the adsorber inlet. Provisions can easily be made to add moisture or gaseous contaminants to the flowing carrier gas stream.

Three adsorbers (either 1-1/4- or 2-in. inside diameter aluminum columns) are located within a Webber, Inc., temperature chamber in which a constant temperature (± 1°C) can be maintained (Figure 8). The columns can be used individually or in series to provide adsorber lengths of 2 to 8 ft. The gas flow path contains in-line probes for continuous, remote monitoring of the gas temperature and humidity. Humidity measurements are made with a Panametrics, Inc., Model-1000 aluminum oxide hygrometer capable of measuring gas dewpoints over the range of -110 to +20°C. The system pressure is controlled with a backpressure regulator located in the gas sampling system and is measured at the entrance of the chamber. The total gas flow rate is continuously monitored at the same location with a calibrated laminar flow element.

Gas Sampling System

The adsorber column effluent flows to the gas sampling system (Figure 9). The total effluent gas flow is diverted into parallel streams so that a portion of the stream can be analyzed in real time at the GC and other fractions can be stored for subsequent analysis. Two 15-loop sample storage valves (S1, S2) are used to store up to thirty 20 cc samples. The volumes of the connecting lines between the GC sample valve (V1) and the 8-port switching valves (C1, C2) have been adjusted to 20 cc to provide a second sample loop for real-time GC analyses. Before the storage valves are indexed to the next sample loop, solenoid valves (E1, E2) are energized to close the inlet lines and enable the loop pressures to bleed down to atmospheric pressure. Check-valves in each of the parallel sample lines prevent the high pressure carrier gas contained within previously analyzed sample loops from diluting subsequent samples. Flows of 40 to 60 cc(STP)/min are maintained through each of the sample loops, requiring a minimum adsorption system backpressure of 1.5 to 2.0 psig.

V. Experimental

Experimental Conditions

Samples of activated carbon from several vendors were evaluated for Kr and Xe adsorption at a variety of test conditions. For all these tests, the carbon was first dried in a 120°C oven purged with dry air to a moisture content of less than 0.3% by weight before loading into the adsorber columns. The carbon was transferred from the oven to a tared adsorber column in less than 2 minutes to minimize moisture pickup. The columns were packed by vibrating the column wall while maintaining a head of several inches of excess carbon above the column top. The columns were then sealed and reweighed.

Before starting a test, the carbon was flushed with dry air(-70°C dewpoint) until the inlet and outlet humidities were equal. After the Kr or Xe run mix was added to the carrier air stream, the column effluent was sampled and analyzed for Kr or Xe. Plotting the measured outlet concentration versus time gives an S-shaped adsorption breakthrough curve (Figure 10). The time axis in Figure 10 is normalized with respect to the mean breakthrough time and the concentration axis with respect to the inlet concentration. The total gas flow rates used in the test program were such that the superficial gas velocity (u) ranged from 0.8 to 3.2 ft/min. The combination of column lengths and flow rates was chosen so that complete breakthrough of the noble gas occurred in a reasonable period of time. For example, at 25°C and at a superficial velocity of 1.6 ft/min, mean holdup times of approximately 25 to 30 minutes and 7 to 8 hours were found for Kr and Xe adsorption, respectively, in a 2-ft long adsorber bed.

Reproducibility

Early in the experimental program, a series of adsorption runs was made to determine error limits and experimental accuracy. Five months later, in tests made with a sample of the same type carbon but which was obtained at a later date, lower values obtained for the adsorption coefficient led to retesting the original carbon sample. Thus, experiments have been run with different columns and column lengths, with columns that had been reloaded with previously tested carbon, as well

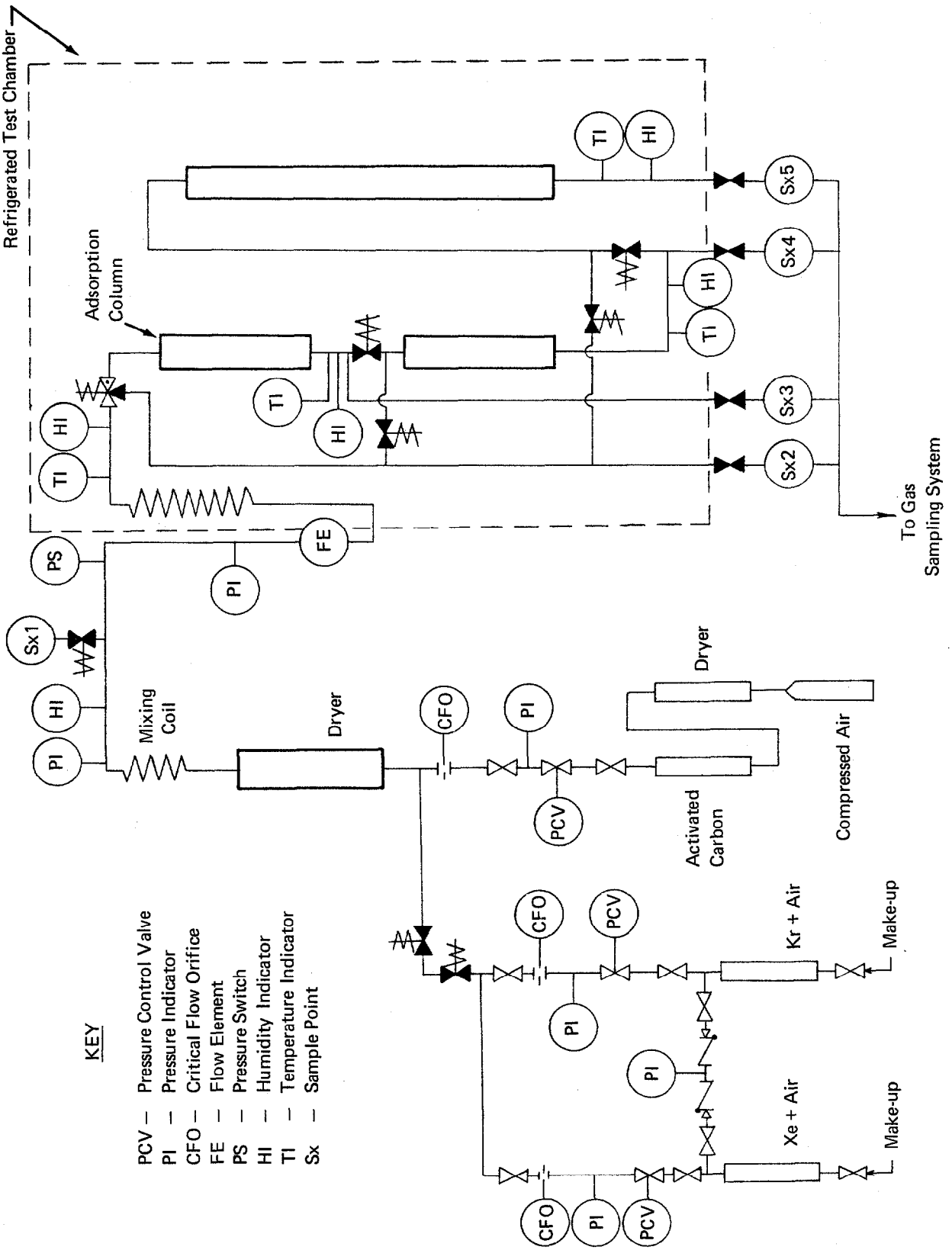

FIGURE 7. EXPERIMENTAL SYSTEM FOR DYNAMIC ADSORPTION MEASUREMENTS

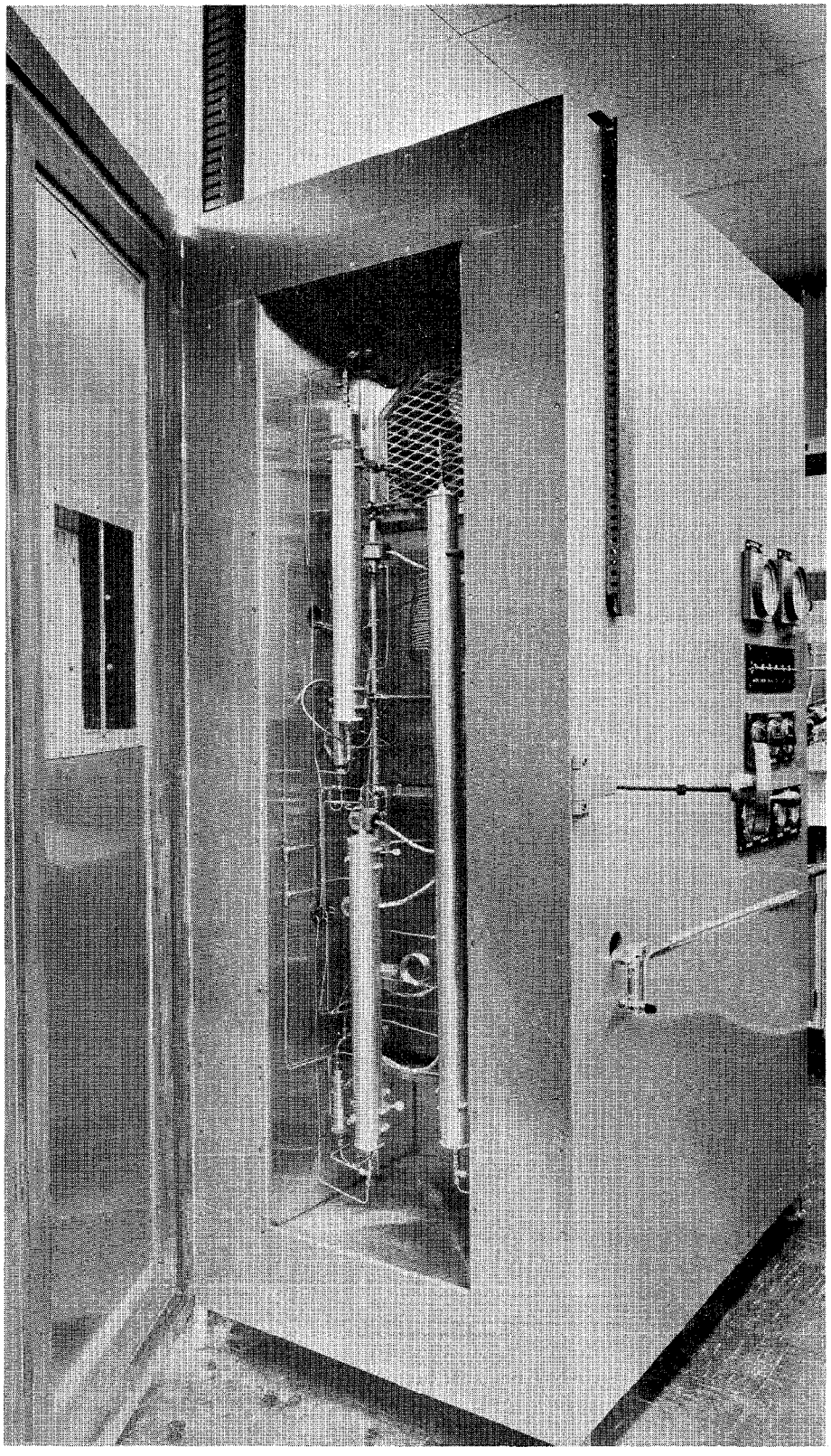

FIGURE 8. ADSORPTION COLUMNS IN CONTROLLED TEMPERATURE CHAMBER

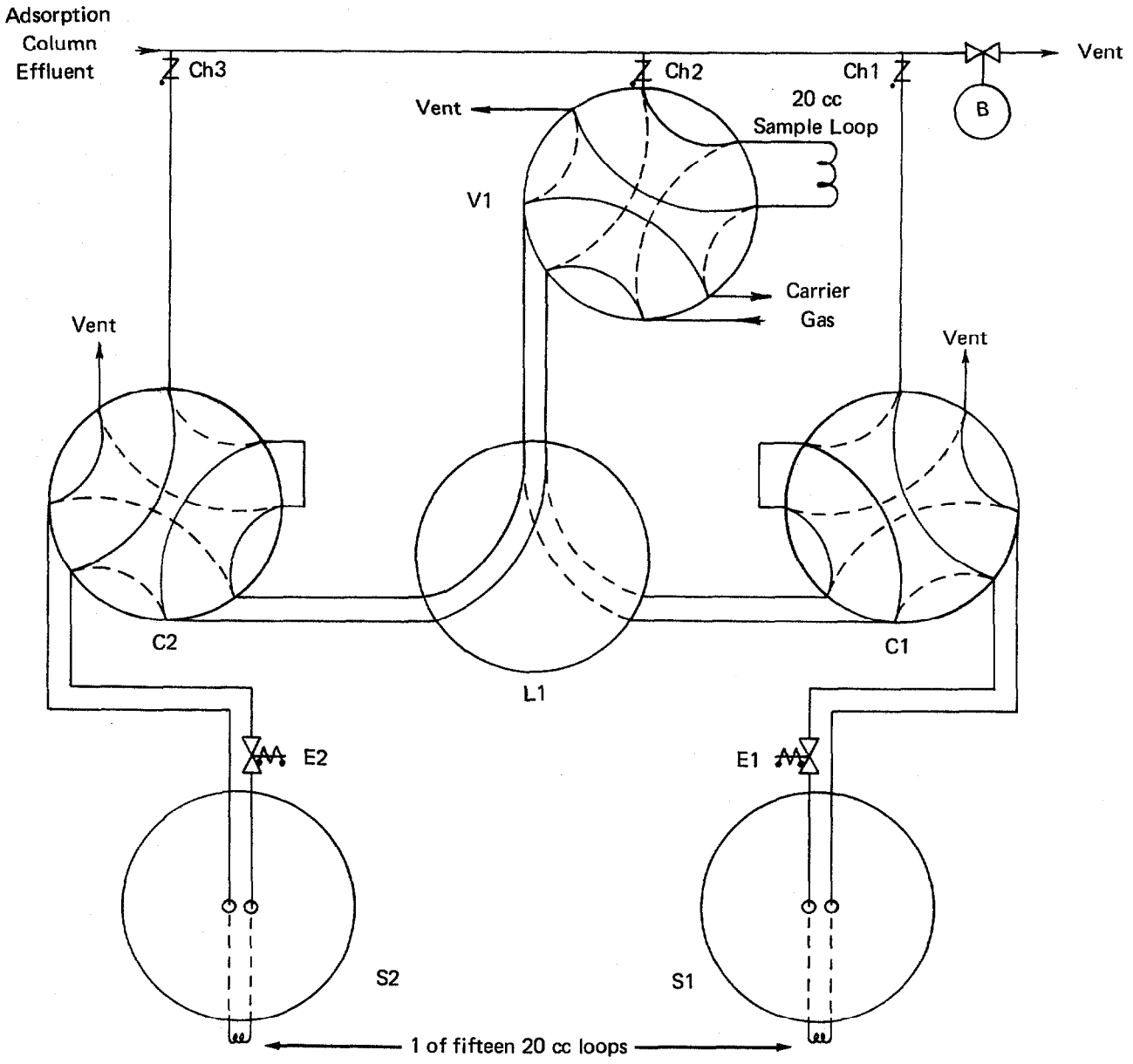

S — 15-loop sample storage valve
C — 8-port switching valve
L — 6-port switching valve
V — 8-port GC sampling valve
Ch — Check valve
E — 2-way solenoid valve
B — Back pressure regulator

FIGURE 9. GAS SAMPLING SYSTEM

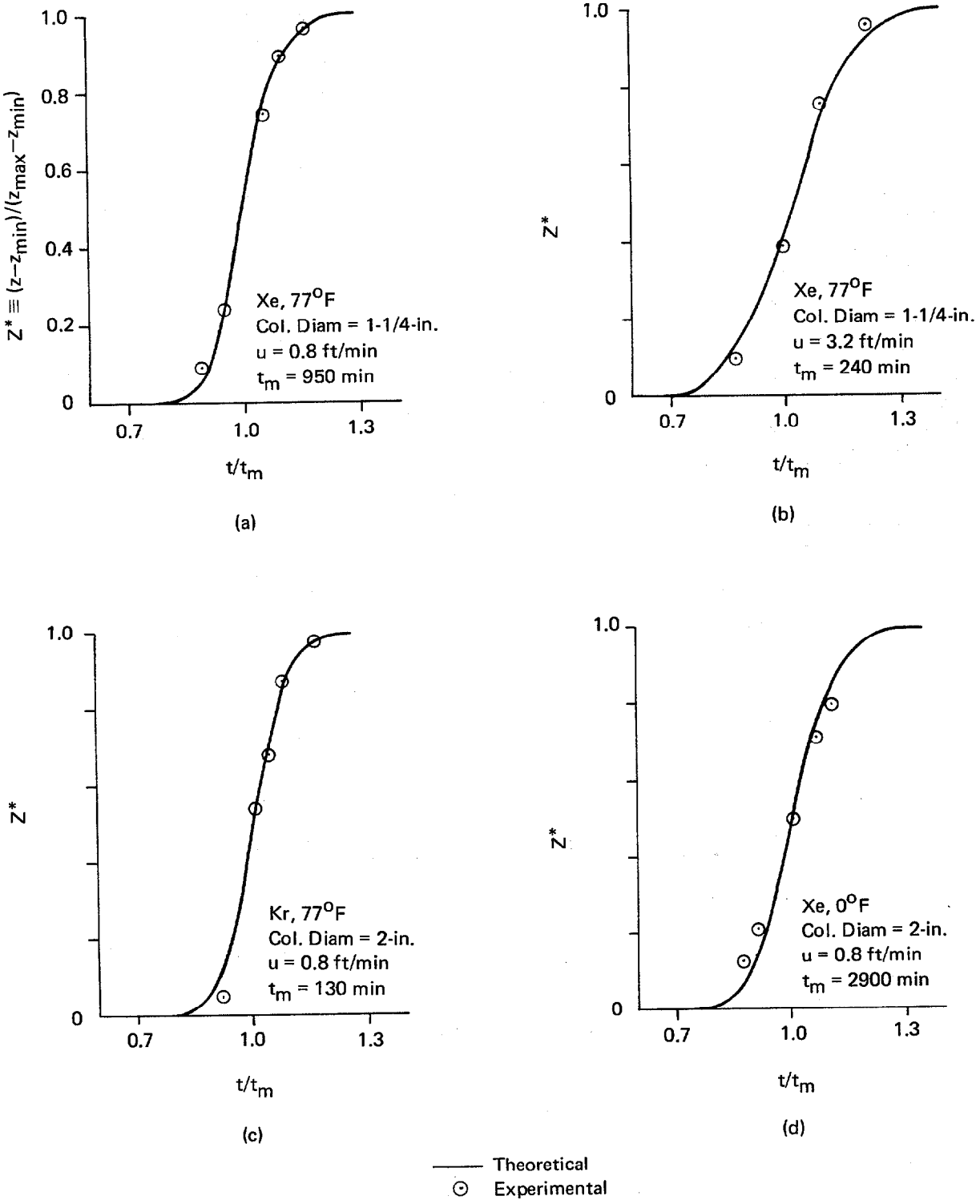

FIGURE 10. CALCULATED VERSUS EXPERIMENTAL BREAKTHROUGH CURVES

as with carbon of the same type received at different times. The results, presented in Table 3, show the combined experimental errors cause less than a ± 3% standard deviation in the calculated dynamic adsorption coefficient.

As shown in Table 3, there was no detectable effect on the dynamic adsorption coefficient of a fourfold change in flow rate (0.8 to 3.2 ft/min) or a twofold change in column cross-sectional area (1-1/4- to 2-in. inside diameter columns). The shape of the breakthrough curves resulting from the different experimental conditions is predicted well by the theory (Figure 10).

TABLE 3. Experimental Reproducibility

Conditions			
Column Size (inches)	Flow Velocity (ft/min)	k_d(Kr)* [cc(STP)/gm]	k_d(Xe)* [cc(STP)/gm]
Coconut Base Carbon A – Sample 1			
1-1/4 X 48	1.6	57.5	
1-1/4 X 96	1.6	55.0	
1-1/4 X 96	1.6	54.0	
1-1/4 X 24	1.6		900
1-1/4 X 48	1.6	55.0	
1-1/4 X 24 (Rerun 5 months after above experiments)	3.2		890
Coconut Base Carbon A – Sample 2			
2 X 48	0.8	52.6	
2 X 24	0.8		775
1-1/4 X 24	0.8		760
1-1/4 X 24	3.2		815
1-1/4 X 24	3.2		790

*k_d measured at 25°C, 16.2 to 16.7 psia and normalized to STP.

Effect of Adsorbate Concentration

One of the goals of this program was to determine the noble gas dynamic adsorption coefficients at conditions approximating those expected in the recombined offgas (primarily air) of an operating BWR. Adsorption experiments were conducted at noble gas concentrations of 1 and 10 ppm. Since atmospheric air contains 1.14 ppm Kr, the columns were first flushed with nitrogen for the low concentration experiments. Changing the noble gas concentration from 1 to 10 ppm produced no noticeable effect on the dynamic adsorption coefficient. Therefore, most experiments were performed with noble gas concentrations of about 10 ppm to simplify the experiments and afford better accuracy.

Effect of Temperature

The capabilities of the controlled temperature chamber containing the adsorber columns permitted experiments to be made over a wide range of temperatures. Although most of the experiments were run at 25°C, some tests were performed at lower temperatures. A comparison of the experimentally measured effect of temperature on the adsorption coefficient for one coconut base carbon with literature data[6-8] (a compilation of several carbon types) is given in Figure 11. It can be seen the experimental and literature adsorption coefficients agree reasonably in absolute value.

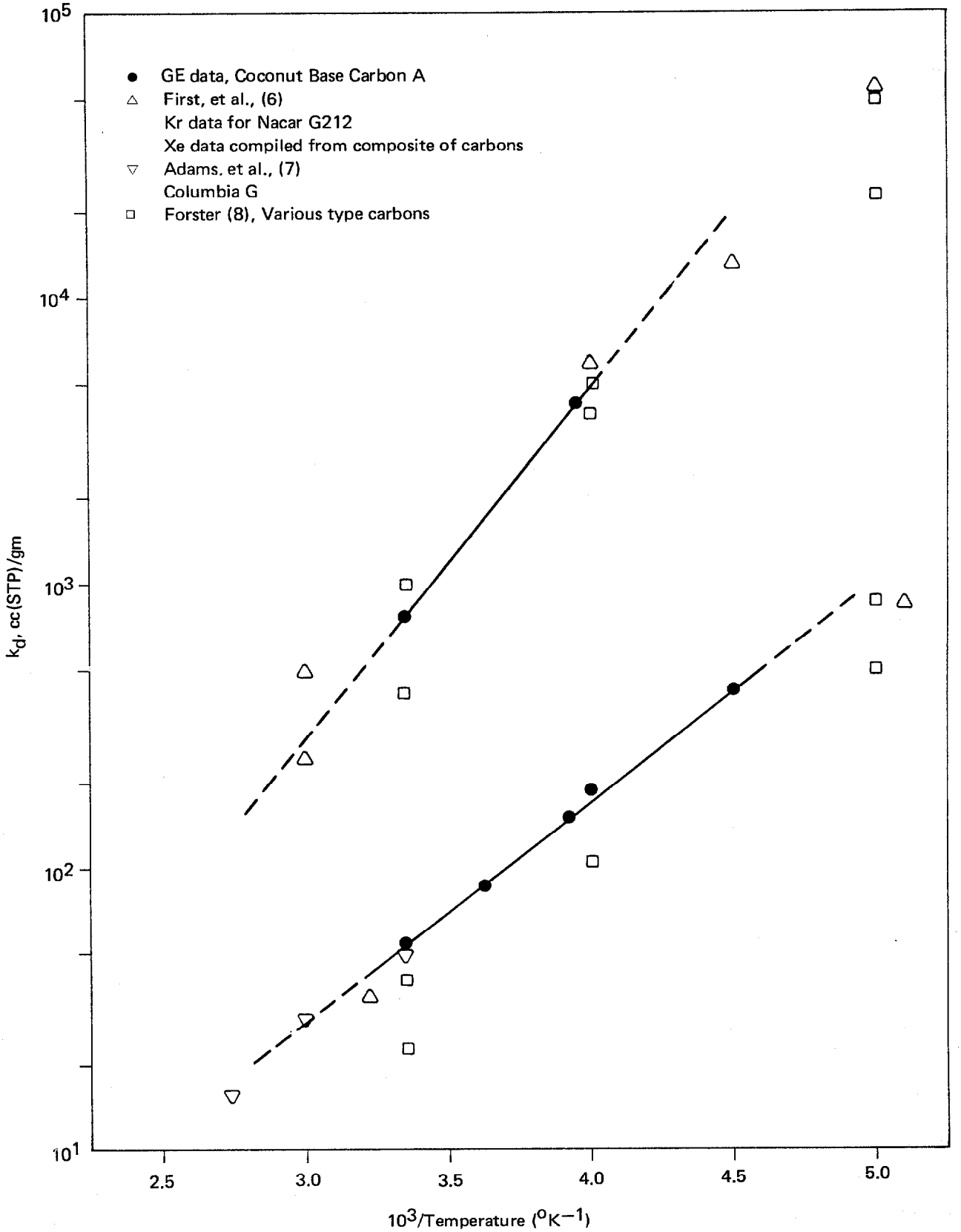

FIGURE 11. DYNAMIC ADSORPTION COEFFICIENT VERSUS TEMPERATURE

Carbon Comparison

The dynamic adsorption coefficients for Kr and Xe have been measured at 25°C on ten different activated carbons. The samples tested included coconut, coal, and petroleum base carbons. As shown in Table 4, the coconut base carbons generally had higher adsorption coefficients. Also, since the ratio of the Xe and Kr dynamic adsorption coefficients for this grouping of carbon samples was fairly constant, a fair prediction of both coefficients might be made on the basis of a single adsorption experiment on each carbon.

TABLE 4. Dynamic Adsorption Coefficients for Selected Carbons
(25°C, Dry Carbon)

	k_d(Kr)*	k_d(Xe)*	k_d(Xe)/k_d(Kr)
	[cc(STP)/gm]		
Coconut Base			
Carbon A	55.3 – 52.6**	910 – 785**	16.4 – 15.8
Carbon B	50.2	770	15.4
Carbon C	57.7	925	16.0
Carbon D	55.5	970	17.4
Carbon E	44.0	690	15.7
Petroleum Base			
Carbon F	47.2 – 46.5**	680 – 655**	14.4 – 14.1
Carbon G	47.7	620	13.1
Carbon H	45.0	720	16.0
Coal Base			
Carbon I	41.9	680	16.3
Carbon J	34.4	460	13.5

*k_d measured at 25°C, 16.7 psia and normalized to STP.
**k_d measured on carbon samples received at different times.

VI. Conclusions

Analytical and experimental techniques have been developed to determine noble gas dynamic adsorption coefficients on activated carbon at concentration levels approximating those in the offgas of an operating BWR. The data obtained agree well with values obtained by other techniques.[6-8] The versatility of the system and procedures developed will enable dynamic adsorption experiments to be conducted with a variety of adsorbate and adsorbent combinations and experimental conditions. The use of nonradioactive gases precludes the need for special safety and monitoring facilities or procedures.

Acknowledgment

The authors wish to acknowledge the efforts of W. R. Kassen and E. J. Jacklitsch in the procurement of the analytical and experimental equipment and of F. A. Arlt and L. R. Powell who assembled the experimental system. In addition, the contribution of F. A. Arlt in conducting the individual tests and maintenance of the equipment is gratefully appreciated.

References

1. Browning, W. E., and Bolta, C. C., "Measurement and Analysis of the Hold-up of Gas Mixtures by Charcoal Adsorption Traps," ORNL-2116, 1956.

2. Robell, A. J., and Merrill, R. P., "Gaseous Contaminant Removal by Adsorption: II. Adsorption Dynamics in Fixed Beds," CEP Symposium Series, No. 96, Vol. 65 (1969).

3. Noble, E. W., Able, K., and Cook, P. W., "Performance and Characteristics of an Ultrasonic Gas Chromatograph Effluent Detector," Analytical Chemistry, 36 1421 – 1427 (1964).

4. Todd, T., and DeBord, D., "An Unconventional Chromatograph for Trace Gas Analysis," American Laboratory, 2, 12, 56 – 61 (1970).

5. Grice, H. W., and David, D. J., "Performance and Applications of an Ultrasonic Detector for Gas Chromatography," Journal of Chromatographic Science, 7, 239 – 247 (1967).

6. First, M. W., et al., Semi-Annual Progress Report (9/8/70–2/28/71), NYO-841–24, prepared for USAEC under Contract AT(30-1)-841. Harvard Air Cleaning Laboratory, Boston.

7. Adams, R. E., et al., "Containment of Radioactive Fission Gases by Dynamic Adsorption," Industrial and Engineering Chemistry, 51, 12, 1467 (1959).

8. Forster, K., "Delaying Radioactive Fission Product Inert Gases in Cover Gas and Off-Gas Streams of Reactors by Means of Activated Charcoal Delay Lines," Kerntechnik, 13, 5, 214 (1971).

DISCUSSION

STEWART, J: How similar is this gas stream to that you would experience from the steam jet air ejector from a boiling water reactor, especially with regard to the concentration of carbon dioxide?

NEULANDER: We are using air, and the steam jet air ejector effluent is essentially air. We have the capabilities of investigating various gas impurities and we have been looking at other gas contaminents, such as carbon dioxide, over a wide range.

STEWART, J: Off hand, what was the concentration of carbon dioxide?

NEULANDER: About 330 ppm; normal air concentration.

BINFORD: What is the effect of humidity on the holdup time?

NEULANDER: We are investigating the effects of humidity. Various people, e.g., Forster in Germany and people here at ORNL, have been investigating the effects of humidity and it does lower the dynamic adsorption coefficient. There are some discrepancies as to how much. The percent reduction is essentially dependent upon the amount of moisture on the carbon.

BINFORD: You are planning to look at that?

NEULANDER: Yes, we are.

THE EFFECT OF HIGH PRESSURE AND LOW TEMPERATURE ON THE ADSORPTION OF XENON AND KRYPTON FROM HELIUM AND ARGON STREAMS*

Ronald S. Ratney**
Dwight W. Underhill
Harvard School of Public Health
665 Huntington Avenue
Boston, Massachusetts 02115

Abstract

The dynamic adsorption coefficients of krypton on activated charcoal from streams of argon and helium was measured at temperatures from -140°C to 0°C and at pressures from 15 psig to 135 psig. Xenon was studied only at 37°C because measurements were not practicable at low temperatures. The adsorption coefficient is considerably higher from helium streams than from argon at all temperatures and pressures studied, and in both cases it increases markedly as the temperature is decreased. Increased pressure causes a proportional increase in adsorption coefficient and the slope of the coefficient-pressure line increases as the temperature decreases with helium as the carrier. With argon, the slope is small and relatively unaffected by temperature above -120°C. At -120°C pressure has almost no effect on the adsorption coefficient and at -140°C the coefficient decreases markedly with increasing pressure up to about 75psig and then increases gradually above that.

* The work reported upon herein was performed under terms of Contract AT(30-1) 841 between Harvard University and the U. S. Atomic Energy Commission.

** Present address: 167 Old Billerica Road
Bedford, Massachusetts 01730

I. Introduction

Adsorption on charcoal is commonly used to remove rare gas fission products from reactor off-gases and cover gases. Systems now in use operate at a number of different temperatures from as low as -150°C to about 50°C, but most of them are used at or near atmospheric pressure. Information is needed on the adsorption capacity of charcoal at high pressures either for the design of holdup beds or for the evaluation of the safety hazards of pressure buildup in atmospheric pressure systems. On request from the USAEC, we carried out experimental measurements for the design of a cover gas clean up system for the FFTF.

This investigation was initiated to study the simultaneous effect of high pressure and low temperature on the adsorption of krypton and xenon from argon and helium carrier gas streams. Förster (1) has reported that the dynamic adsorption coefficient of krypton from argon streams increases monotonically at temperatures as low as -50°C, but it was thought that competition between carrier and fission gas might result in increased pressure causing a decrease in adsorption capacity at very low temperatures(2). Accordingly experiments were done at temperatures extending below the critical point of argon (-122°C) and as shown below, increased pressure does indeed cause decreased adsorption capacity at -140°C. This is an important finding for the design of fission gas adsorption beds.

II. Apparatus

Following the initial request for test data we were able to assemble a complete system from commercially available equipment. A schematic diagram and photograph of the system are shown in Figures 1 and 2. The adsorption column was a short length of iron pipe containing Pittsburgh PCB charcoal. In most of the experiments, the column was 2" long by 5/8"i.d.(5.08 x 2.19 cm) although smaller or larger columns were used for some experiments. The mesh size was usually 6 x 16 but here too, a few experiments were done with finer material. The results did not seem to be affected by variations in mesh size. The temperature within the bed was measured with a steel clad copper-constantan thermocouple inserted into the center of the column along the axis. The potential produced by the thermocouple was measured with a Leeds and Northrup potentiometer using an ice bath as the reference. The thermocouple voltage was measured several times during a run and the average voltage was converted to a temperature by interpolating in a calibration table. During a run, the thermocouple voltage rarely varied by more than 0.01 mv which corresponds to a temperature variability of about 1°C. After the column had been packed with charcoal, it was baked out at 110°C for several hours to remove moisture.

The constant temperature chamber was a styrofoam box into which liquid nitrogen was sprayed. A solenoid valve on the liquid nitrogen reservoir was turned on and off by a thermostatic controller which sensed the temperature in a chamber with a copper-constantan thermocouple. The temperature in the chamber varied by a few

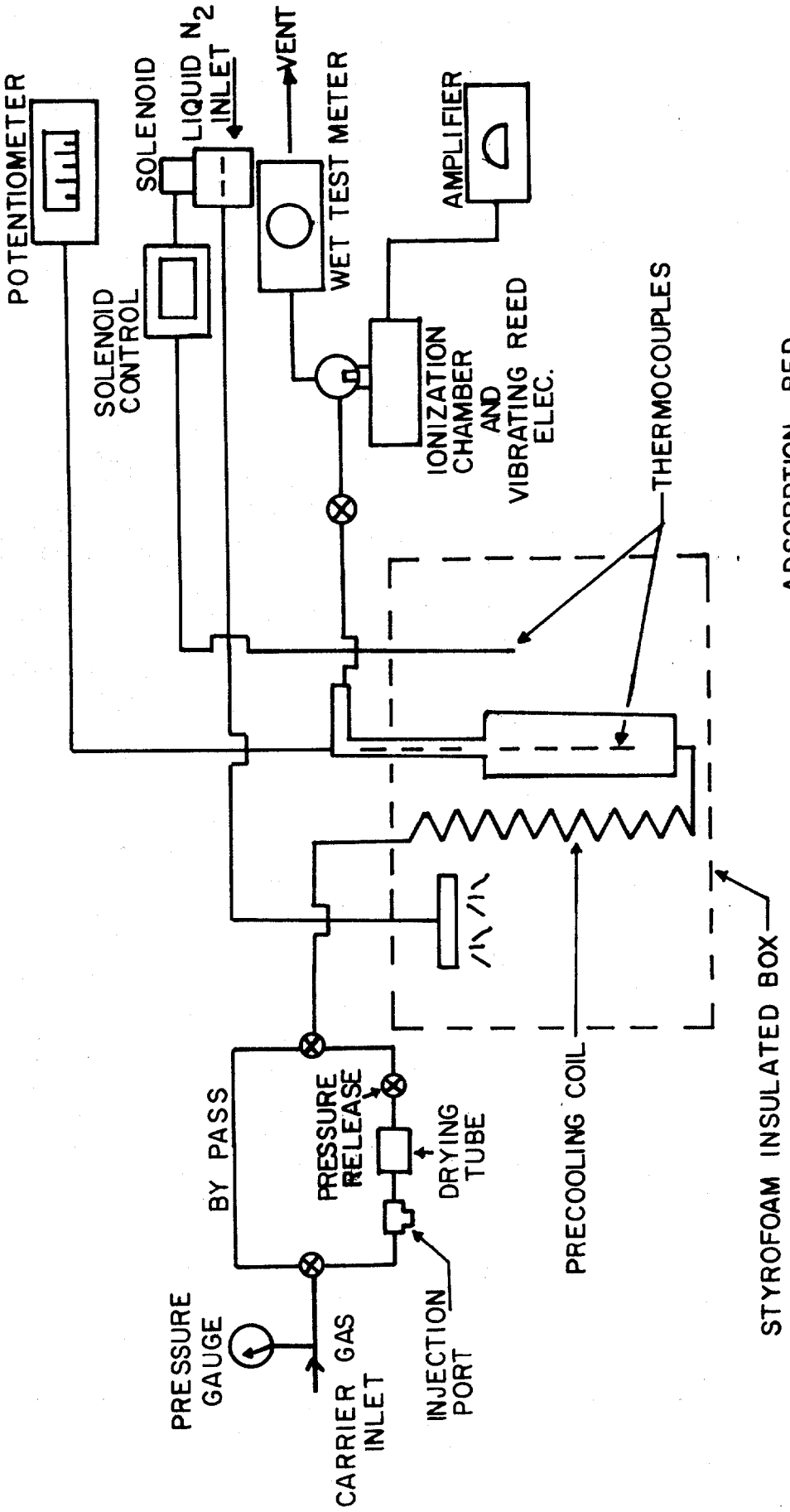

FIGURE I. DIAGRAM OF TEST APPARATUS.

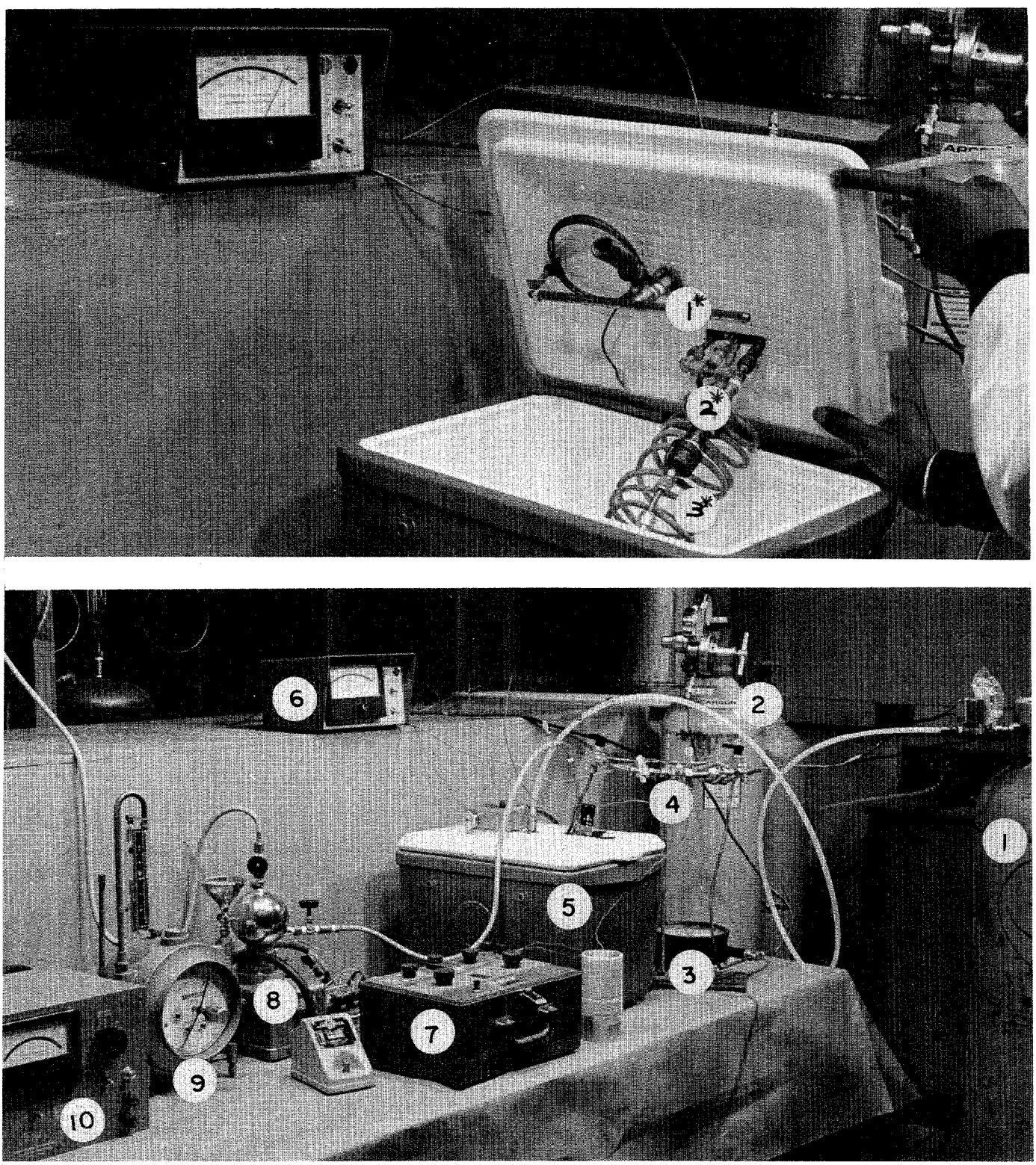

Figure 2. Apparatus for determining adsorption coefficients at elevated pressures and reduced temperatures. *1-nitrogen spray head; *2-adsorption column; *3-carrier gas precooling coil; -- 1-liquid nitrogen source; 2-carrier gas source; 3-pressure gauge; 4-injection system; 5-low temperature chamber; 6-low temperature controller; 7-potentiometer for column thermocouple; 8-ionization chamber; 9-wet test gas meter; 10-electrometer for ionization chamber.
*Close up view.

degrees during a run, but the thermal mass of the column smoothed out these variations. Gas being fed to the column was precooled by passage through a ten-foot coil of copper tubing.

Carrier gas pressure was controlled with a Matheson high pressure regulator and measured with a Bourdon gauge. No variations in pressure were noted during a run. The accuracy of the pressure gauge was judged to be about 0.5 psi. Gas flow was controlled by a miniature needle valve at the outlet to the column. Total gas volume was read from the wet test meter at intervals and the flow rate was calculated from the time-volume data. The flow rate was found to be constant to within the accuracy of the measuring equipment.

The concentration of radioactive krypton or xenon in the carrier stream was measured by passing it through a 500 ml spherical ionization chamber which had a DC potential of 127 volts across it. The ionization current which is directly proportional to the activity of the gas stream was measured with a Cary vibrating reed electrometer.

In order to avoid injecting samples into the pressurized system, a bypass was set up that allowed carrier gas to continue flowing under pressure while the sample was injected at atmospheric pressure. Then valves were switched to pick up the sample in the pressurized stream.

III. Procedure

Before injecting a sample for a run, the temperature, pressure, and flow rate were stabilized. The flow rate was adjusted to 0.3-1.5 liters per minute although it has been shown (3) that flow rate is not critical. No attempt was made to set it at a particulate value.

Radioactive krypton-85 and xenon-133 were obtained as solution in physiological saline. These solutions are commonly used as diagnositc reagent in lung disease and are inexpensive sources of these isotopes. To start a test run, 0.1 ml of the solution was drawn into a 1 ml syringe. Then about 0.9 ml of carrier gas was drawn into the syringe, the gas freed from the solution by agitation, and the gas phase was then injected. A drying agent in the gas line removed traces of moisture before the sample reached the adsorption bed.

Every minute or so after the injection, the electrometer current and elapsed time were recorded. Soon after injection, the electrometer current rose rapidly to a peak value and then decreased exponentially. Since the exponential decay was regular, the electrometer current was recorded only until it reached 1-5% of the peak value. It was then extrapolated to the point where it was less than 1 ma.

IV. Data Analysis

All of the data from a run was punched onto IBM cards for analysis by computer. A program was written which calculated the average temperature and flow rate, converted the elapsed time readings to volumes and wrote the entire record of an experiment

on magnetic tape for later analysis. Dynamic adsorption coefficients were calculated from the elution curves by moment analysis[4].

Results

The adsorption of xenon from argon or helium streams was studied only at 38°C. At temperatures below zero, the adsorption coefficients were so high that complete elution curves could not be obtained within one working day. The results are shown in Figure 3. The straight lines drawn through the sets of points were placed visually. With krypton, experiments could be run at temperatures as low as -160°C although -140°C was the lowest temperature used in routine experiments. Argon boils at -186°C at one atmosphere and at -160°C at seven atmospheres. In normal operation, the cold chamber was about twenty degrees colder than the adsorption bed, and when the column was operated at much below -140°C, argon would occasionally condense in the precooling coil and cause erratic pressure variations. The lowest temperature used with helium as the carrier gas was -78°C. Below this point, the adsorption coefficient became so large that complete elution curves could not be otained in a reasonable time.

Plots of the adsorption coefficients vs. the reciprocal of the absolute temperature are shown in Figures 4 and 5. The plot shown in figure 4 was obtained by least squares analysis of the results of 116 experiments using argon as the carrier gas. Actually different regression lines should have been obtained for different pressures, but they were indistinguishable within the accuracy of the experiments. With helium as the carrier gas, the adsorption coefficients varied much more with pressure so that separate plots could be constructed for each pressure as shown in Figure 5.

Figures 6 and 7 show the effect of pressure on the adsorption of krypton from helium and argon streams at various temperatures. The results shown for -140°C were obtained with charcoal with a slightly lower adsorptive capacity. The following points should be noted.

1. The adsorption coefficients are uniformly higher when helium is used as the carrier gas.

2. The effect of pressure is much more marked with helium.

3. Perhaps the most important observation that can be made is that the adsorption coefficient of krypton from argon streams increases with pressure at temperatures above -120°C; is almost unaffected by pressure at -120°C, and at -140°C actually decreases markedly over the range of 15-75 psig.

FIGURE 3. EFFECT OF PRESSURE ON THE DYNAMIC ADSORPTION COEFFICIENT OF XENON ON PCB 6X16 MESH CHARCOAL AT 38° C.

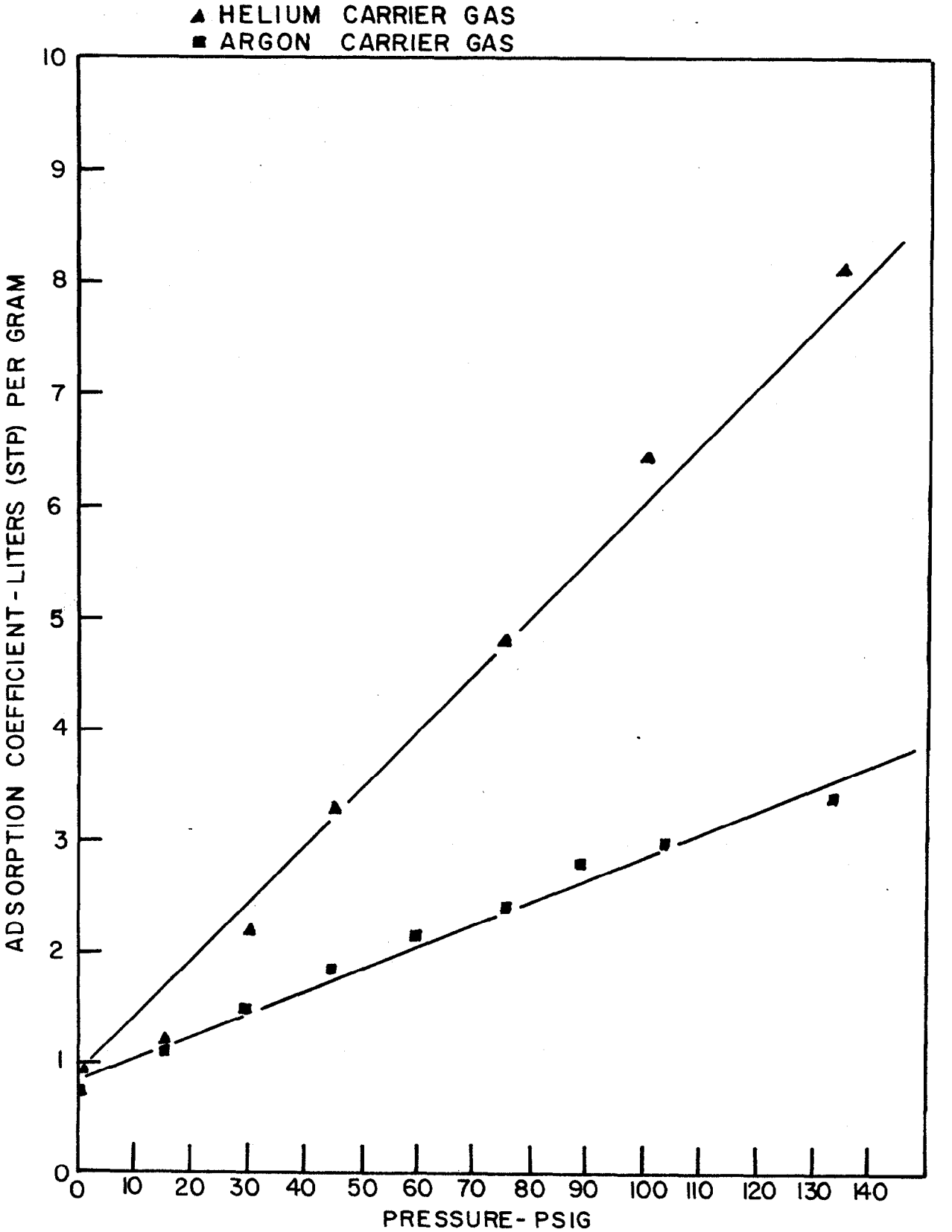

FIGURE 4. EFFECT OF TEMPERATURE ON THE DYNAMIC ADSORPTION OF KRYPTON ON CHARCOAL FROM ARGON STREAMS.

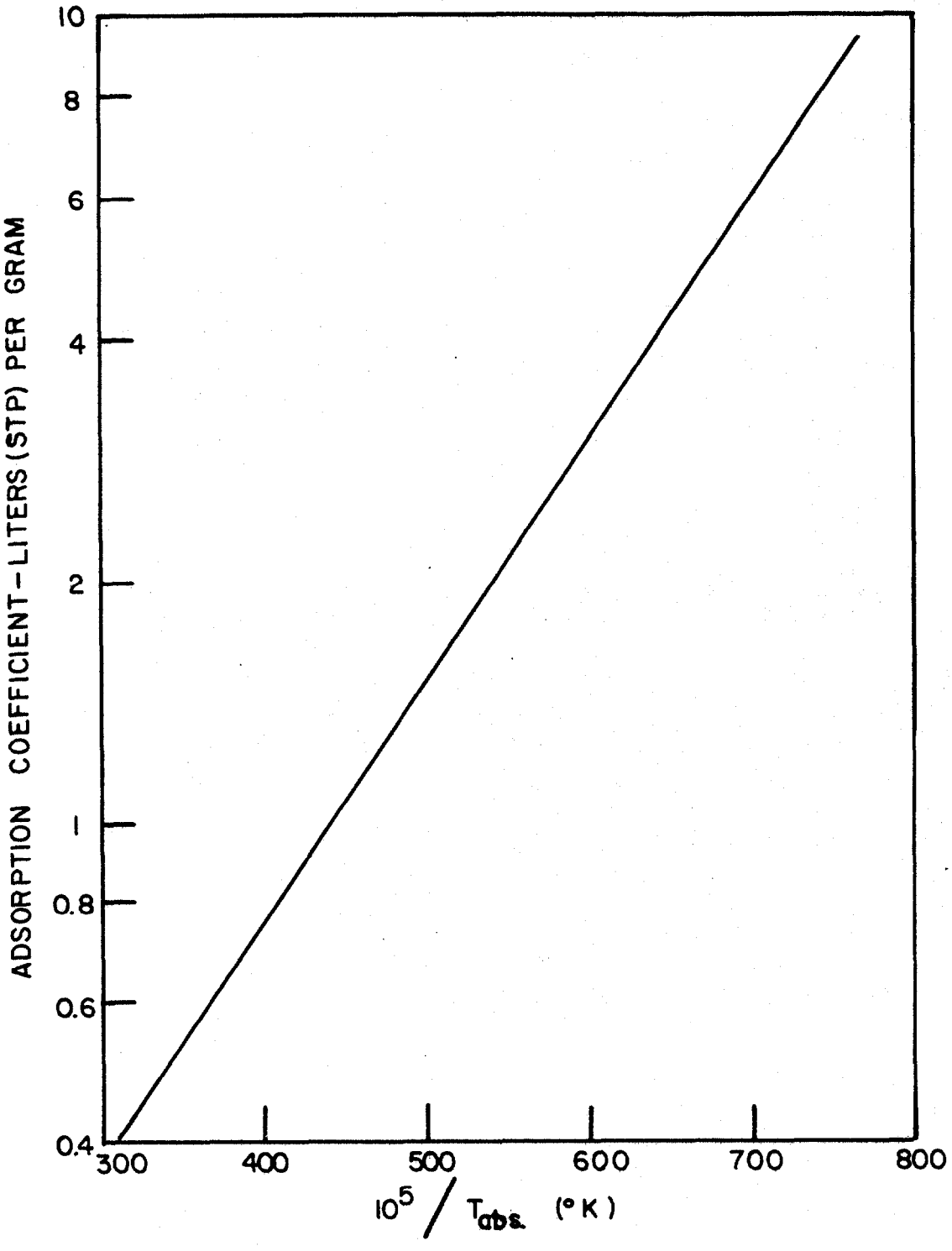

FIGURE 5. EFFECT OF TEMPERATURE ON THE ADSORPTION OF KRYPTON ON CHARCOAL FROM HELIUM STREAMS.

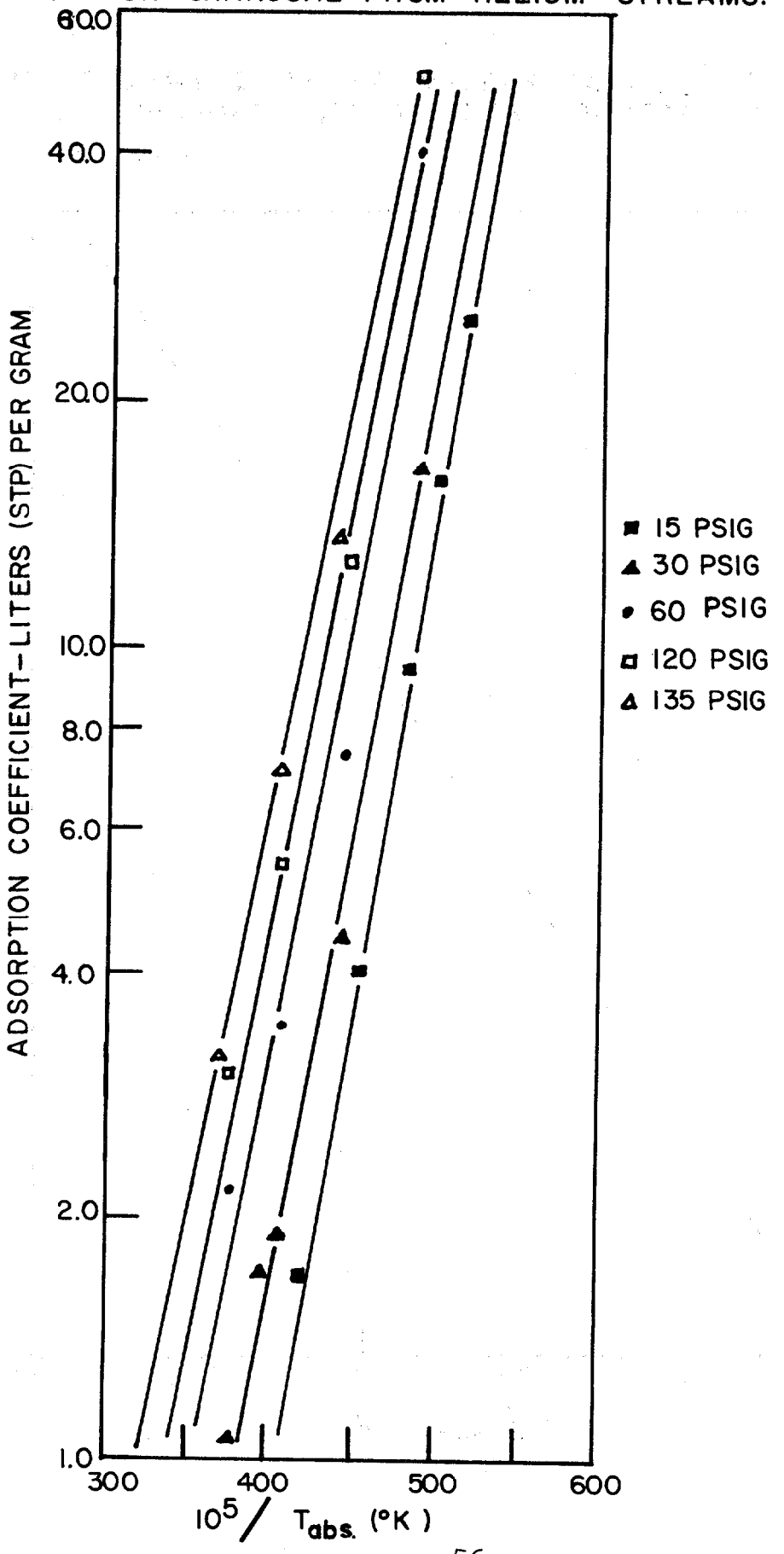

FIGURE 6. DYNAMIC ADSORPTION COEFFICIENT OF KRYPTON ON P.C.B. 6 X 16 MESH CHARCOAL FROM ARGON CARRIER STREAMS

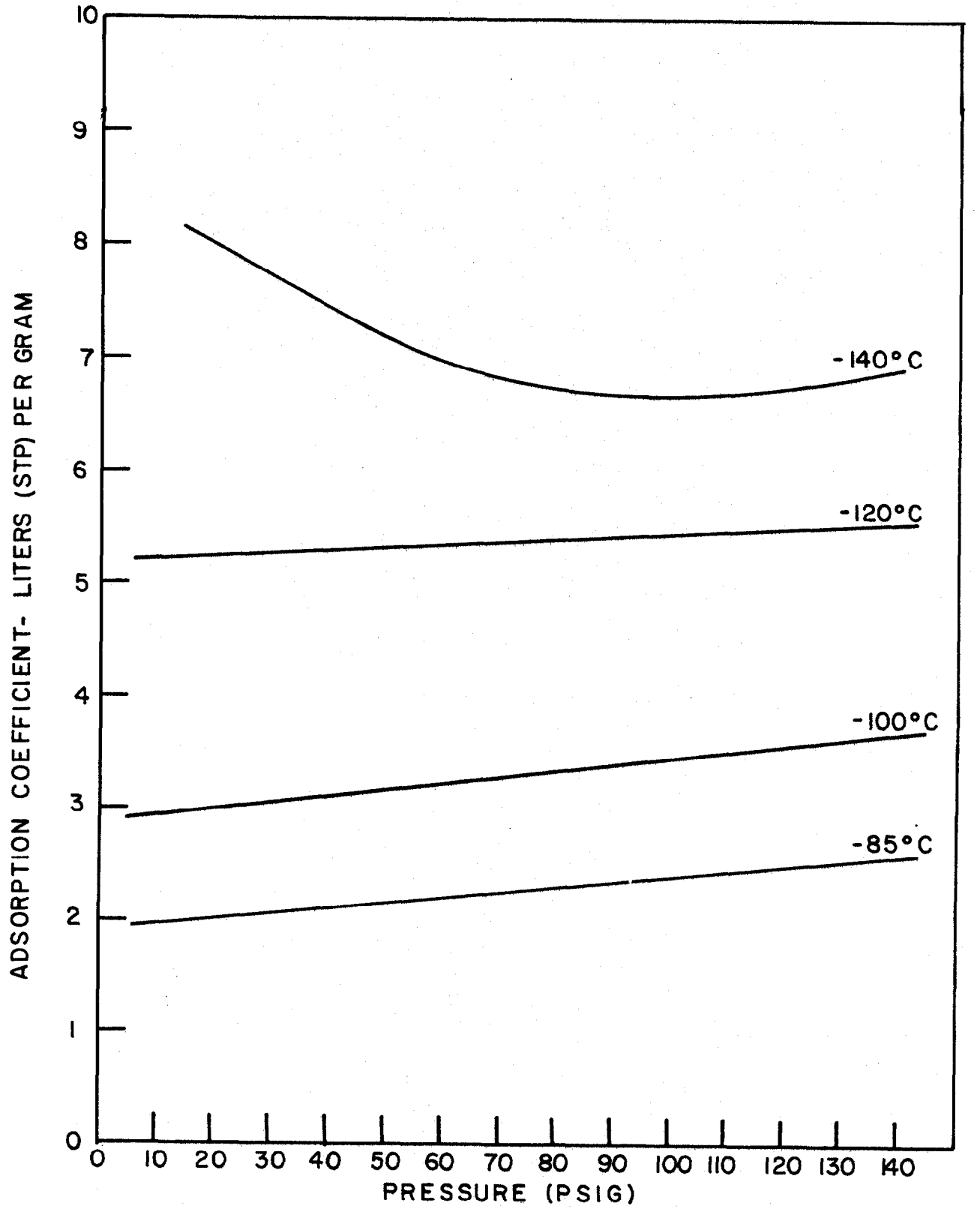

FIGURE 7. DYNAMIC ADSORPTION COEFFICIENT OF KRYPTON ON PCB 6 X 16 MESH CHARCOAL FROM HELIUM CARRIER STREAMS.

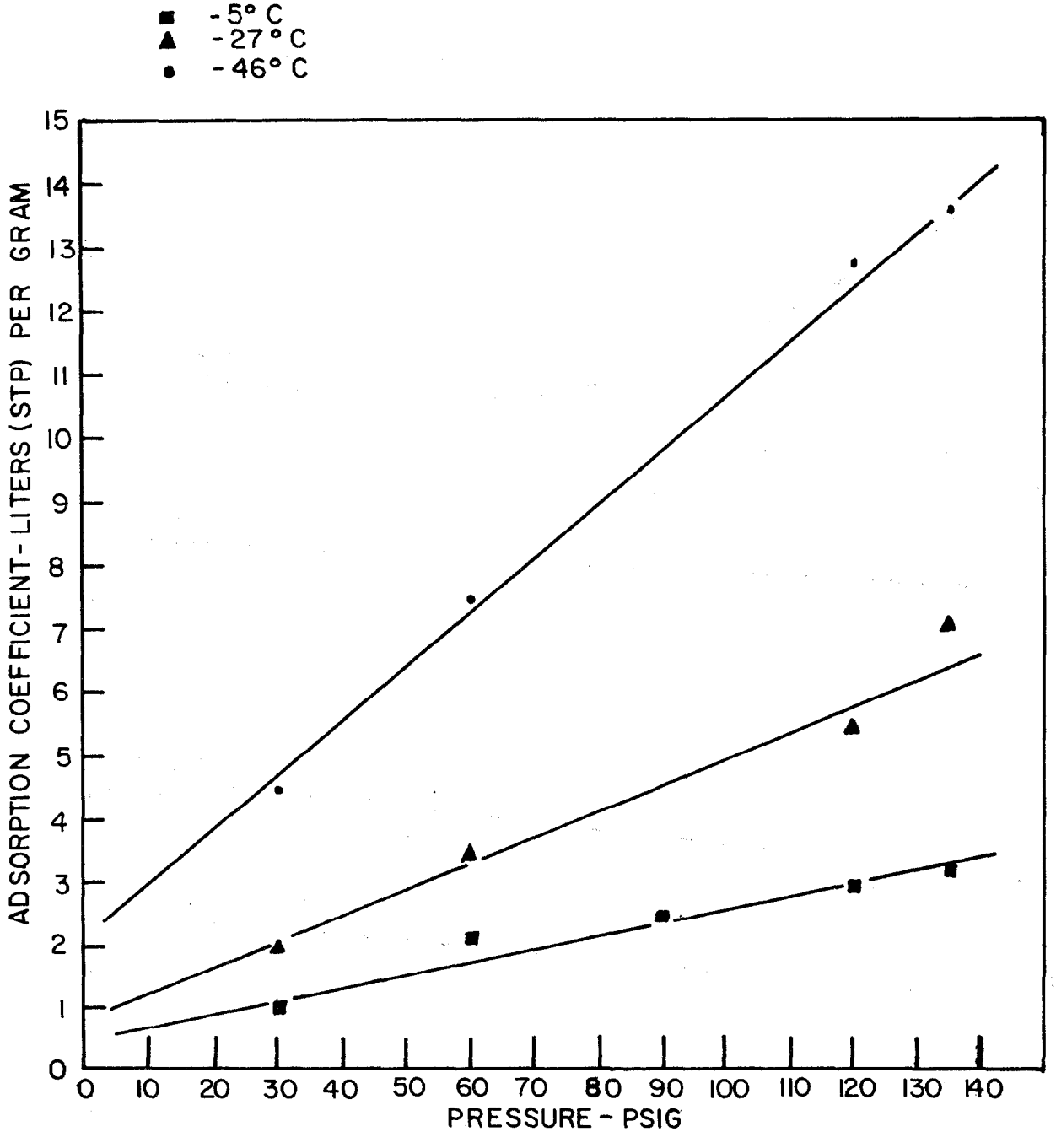

Discussion

The results reported here generally confirm those obtained by Förster[1]. He observed the effect of temperature on the dynamic adsorption coefficient and also that temperature had a greater effect with helium as the carrier gas. He also notes that the coefficient increases with pressure although the slope of his curve is higher than that reported here.

It seems significant that the slope of the adsorption coefficient - pressure curve changes from positive to negative around -120°C. The critical temperature of argon is -122°C which means that below this temperature argon is capable of existing as a liquid. According to the BET theory, multilayer adsorption is possible only below the critical temperature and according to Dubinin, the adsorbed phase can be considered to be similar to a liquid below the critical point. Thus above -122°C we are probably observing phenomena associated with the adsorption of krypton and argon on bare carbon surfaces while below this point the situation is more akin to gas-liquid partition. In this region, the parameters that will be needed for a theoretical examination of the data presented here are the solubilities and heats of solution of krypton and xenon in a phase which is similar to, but certainly different from, pure liquid argon.

References

1. K. Förster, Kerntechnik-Atompraxis, 13, 214-219 (1971).

2. M. W. First, D. W. Underhill, J. Tadmor, R. R. Hall, R. S. Ratney, T. W. Baldwin, and D. W. Moeller. Harvard Air Cleaning Laboratory, NYO-841-25. Semiannual Progress Report, March 1, 1971-August 31, 1971 (Issued November, 1971).

3. D. W. Underhill, Nuc. Appl. 6, 544-548 (1969).

4. D. W. Underhill, Nuc. Appl. and Tech., 8, 255-260 (1970).

Acknowledgement

We wish to gratefully acknowledge the expert assistance of Mr. Floyd Hardwick in carrying out the experimental work reported here.